Int J Hematol (2014) 99:21–31
DOI 10.1007/s12185-013-1466-x

ORIGINAL ARTICLE

Bromodomain-PHD finger protein 1 is critical for leukemogenesis associated with MOZ–TIF2 fusion

Haruko Shima · Kazutsune Yamagata · Yukiko Aikawa · Mika Shino · Haruhiko Koseki · Hiroyuki Shimada · Issay Kitabayashi

Received: 29 June 2013 / Revised: 3 November 2013 / Accepted: 5 November 2013 / Published online: 21 November 2013

Abstract Chromosomal translocations that involve the monocytic leukemia zinc finger (MOZ) gene are typically associated with human acute myeloid leukemia (AML) and often predict a poor prognosis. Overexpression of HOXA9, HOXA10, and MEIS1 was observed in AML patients with MOZ fusions. To assess the functional role of HOX upregulation in leukemogenesis by MOZ–TIF2, we focused on bromodomain-PHD finger protein 1 (BRPF1), a component of the MOZ complex that carries out histone acetylation for generating and maintaining proper epigenetic programs in hematopoietic cells. Immunoprecipitation analysis showed that MOZ–TIF2 forms a stable complex with BRPF1, and chromatin immunoprecipitation analysis showed that MOZ–TIF2 and BRPF1 interact with HOX genes in MOZ–TIF2-induced AML cells. Depletion of BRPF1 decreased the MOZ localization on HOX genes, resulting in loss of transformation ability induced by MOZ–TIF2. Furthermore, mutant MOZ–TIF2 engineered to lack histone acetyltransferase activity was incapable of deregulating HOX genes as well as initiating leukemia. These data indicate that MOZ–TIF2/BRPF1 complex upregulates HOX genes mediated by MOZ-dependent histone acetylation, leading to the development of leukemia. We suggest that activation of BRPF1/HOX pathway through MOZ HAT activity is critical for MOZ–TIF2 to induce AML.

Keywords MOZ–TIF2 · BRPF1 · *HOX* genes · AML

H. Shima · K. Yamagata · Y. Aikawa · M. Shino · I. Kitabayashi (✉)
Division of Hematological Malignancy, National Cancer Center Research Institute, 5-1-1 Tsukiji, Chuo-ku, Tokyo 104-0045, Japan
e-mail: ikitabay@ncc.go.jp

H. Shima · H. Shimada
Department of Pediatrics, Keio University School of Medicine, Tokyo, Japan

H. Koseki
Department of Developmental Genetics, RIKEN Research Center for Allergy and Immunology, RIKEN Yokohama Institute, Yokohama, Japan

Introduction

Monocytic leukemia zinc finger protein (MOZ) is a MYST (MOZ, Ybf2 (Sas3), Sas2, Tip60)-type histone acetyltransferase (HAT), and interacts with AML1, PU.1 or p53 to activate transcriptions of their target genes [1–3]. While MOZ plays a crucial role in the maintenance of normal hematopoietic stem cells [4], MOZ is also involved in chromosomal translocations such as t(8;16)(p11;p13), t(8;22)(p11;q13) and inv(8)(p11;q13), resulting in fusions of MOZ–CBP, MOZ–p300 and MOZ–TIF2, respectively, which are associated with acute myelomonocytic leukemia [5–8]. MOZ-related translocations are observed in approximately 1–6.5 % of AML, and indicate poor prognosis [9, 10]. We have previously shown that upregulation of M-CSFR (CSF1R) mediated by PU.1 is crucial for the maintenance of AML stem cells in MOZ–TIF2 leukemia [2]. However, although deletion of *CSF1R* delayed the onset of MOZ–TIF2 leukemia in vivo, approximately half of the mice transplanted with *CSF1R*-deleted, MOZ–TIF2-transduced cells developed leukemia in the long term. This may suggest the presence of another pathway involved in the generation of MOZ–TIF2 leukemia.

To pursue other pathways independent of PU.1/M-CSFR pathway, we focused on *HOX* genes. Enforced

expression of *HOXA9* or *HOXA10* immortalizes bone marrow (BM) progenitors in vitro [11, 12]. However, HOXA9 or HOXA10 overexpressed cells require relatively long latency period to induce leukemia in recipient mice. This may suggest that another complementing mutation would be needed for dominant outgrowth of transplanted cell [13, 14].

HOX genes are upregulated in BM samples of patients with MOZ-related leukemias as well as in BM cells of MOZ–TIF2-induced AML mouse model [2, 15]. MOZ forms complex with ING5 (inhibitor of growth 5), EAF6 (homolog of Esa1-associated factor 6), and BRPF1/2/3 (bromodomain-PHD finger protein 1, 2 or 3), and MOZ is the catalytic component of this HAT complex [9]. Recently, it was reported that BRPF1, a component of the HAT complex is required for the maintenance of HOX genes expression [16, 17]. Because HAT domain is intact in most of the fusions and sufficient for forming HAT complex [9], MOZ fusions may also form complex and deregulate *HOX* genes mediated by BRPF1. This study was performed to determine the role of BRPF1 in the regulation of *HOX* genes, and in the generation of MOZ–TIF2 leukemia.

Fig. 1 Effects of *Brpf1* knockdown on MOZ–TIF2 leukemic cells in vitro. **a** HA-tagged wild-type MOZ–TIF2 was cotransfected into 293FT cells together with FLAG-tagged WT BRPF1, deletion 1–222 (Δ1–222) BRPF1, or empty vector. Immunoprecipitates with anti-FLAG antibody (M2 IP) or cell lysates (Extracts) were subjected to immunoblotting with anti-HA or anti-FLAG antibodies. Δ1–222 BRPF1 lost its ability to coprecipitate with MOZ–TIF2. **b** Efficiency of *Brpf1* knockdown by Brpf1 shRNA on MOZ–TIF2 leukemic cells. RT-PCR analysis for mouse *Brpf1* (*left*) and human *BRPF1* (*right*) of MOZ–TIF2 leukemic cells expressing WT human BRPF1, Δ1–222 BRPF1 or empty vector, after transduction with mouse Brpf1 shRNA. Brpf1 shRNA significantly suppressed the expression level of mouse Brpf1 but not human BRPF1. Data are mean ± SD ($n = 3$). $^{**}P < .01$. **c** Efficiency of *Brpf1* knockdown by Brpf1 shRNA on MOZ–TIF2 leukemic cells. Western blots for both mouse Brpf1 and human BRPF1 in cell lysates from MOZ–TIF2 leukemic cells expressing WT human BRPF1, Δ1–222 BRPF1 or empty vector, after transduction with mouse Brpf1 shRNA. Brpf1 shRNA significantly suppressed the expression level of mouse *Brpf1* but not human *BRPF1*. **d** Relative colony number of MOZ–TIF2 leukemic cells transduced with control shRNA or Brpf1 shRNA. Knockdown of *Brpf1* resulted in reduction of colony formation. Overexpression of WT BRPF1 but not Δ1–222 BRPF1 restored the colony formation activity of cells with downregulated Brpf1. Data are mean ± SD ($n = 3$). $^{**}P < .01$. **e** Effects of Brpf1 shRNA on expression of *Hoxa9, Hoxa10, Meis1* and *BRPF1* in MOZ–TIF2 leukemic cells expressing WT BRPF1, Δ1–222 BRPF1 or empty vector. qRT-PCR showed that the expression level of *Hoxa9, Hoxa10* and *Meis1* was significantly suppressed by Brpf1 shRNA, which was restored by overexpression of WT BRPF1 but not Δ1–222 BRPF1. Data are mean ± SD ($n = 3$). $^{**}P < .01$

Methods

Mice

C57/BL6 mice were purchased from CREA Japan. Mouse experiments were performed in a specific pathogen-free environment at the National Cancer Center animal facility according to institutional guidelines with approval of the National Cancer Center Animal Ethics Committee.

Plasmids

MOZ and MOZ–TIF2 plasmids used here were described previously [1, 2]. Human BRPF1 cDNA was purchased from Openbiosystems and inserted into MSCV-neo vector. Human HOXA9 cDNA was isolated by cloning K562 cells and inserted into MSCV-neo vector. Deletion mutants of MOZ–TIF2 and BRPF1 and point mutants of MOZ were constructed by ligation of the cDNA fragments made by restriction enzymes and PCRs.

Retrovirus transduction and AML mouse model

Plasmid DNA was transfected into PlatE packaging cells using the FuGENE 6 reagent (Roche Diagnostics), and supernatants containing retrovirus were collected 48 h after transfection. c-kit$^+$ progenitors were obtained from BM mononuclear cells using anti-CD117 beads (Miltenyi Biotec.) and incubated with retrovirus in a retronectin (Takara Bio)-coated plate. After 24 h of culture, cells were harvested and transplanted into sublethally irradiated recipient mice. The recipients were monitored for signs of leukemia (i.e., facial edema, lymphadenopathy, moribund, increase of GFP$^+$ cells in peripheral blood).

Colony formation assay

The GFP$^+$ infectants were sorted by cell sorter, and 1×10^4 of cells were cultured in 1 ml of methylcellulose media M3234 (Stem Cell Technologies) supplemented with 10 ng/ml of SCF, 10 ng/ml of IL-3, 10 ng/ml of GM-CSF (Peprotech). Number of colonies was monitored every 5–7 days of each replating using a DMIL inverted contrasting microscope (Leica). Cell sorting was performed using the cell sorter JSAN (Baybioscience). For the experiments using MSCV-neo vectors, infected cells were selected by adding G418 in the culture medium.

Brpf1 knockdown analysis

Brpf1 shRNA in lentiviral vectors was purchased from Openbiosystems. Viral particles were generated by co-transfection of 293FT cells with lentiviral packaging plasmids using Gene Juice (MERCK4Biosciences). $1–2 \times 10^5$ of MOZ–TIF2 leukemic cells were transduced with pLKO.1 vector or pLKO.1-Brpf1 vector by

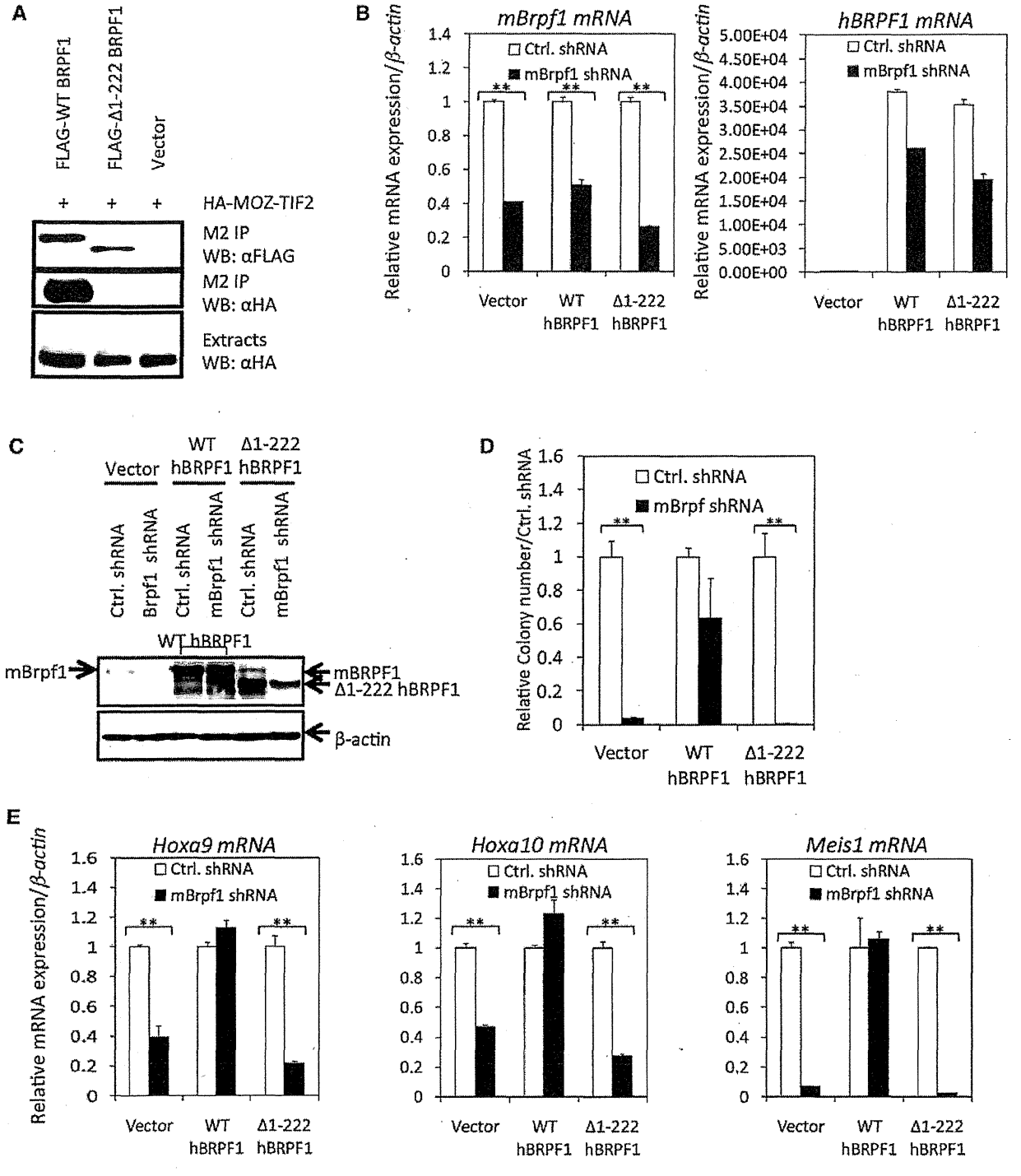

spinoculation at 2500×*g* for 2 h at 32 °C in virus containing medium supplemented with 8 ng/ml of polybrene. The cells were resuspended in StemPro-34 SFM medium (Invitrogen) containing cytokines (20 ng/ml SCF, 10 ng/ml OSM, 10 ng/ml IL-3) for 24 h. The infectants were plated in methylcellulose media supplemented with 10 ng/ml of SCF, 10 ng/ml of IL-3, 10 ng/ml of GM-CSF, in the presence of puromycin (4 μg/ml) for selection of infected cells. Three days after selection with puromycin, 1×10^4 cells were plated in 1 ml of methylcellulose media and were proceeded to colony formation assay. The redundant infectants were used for qRT-PCR assay and

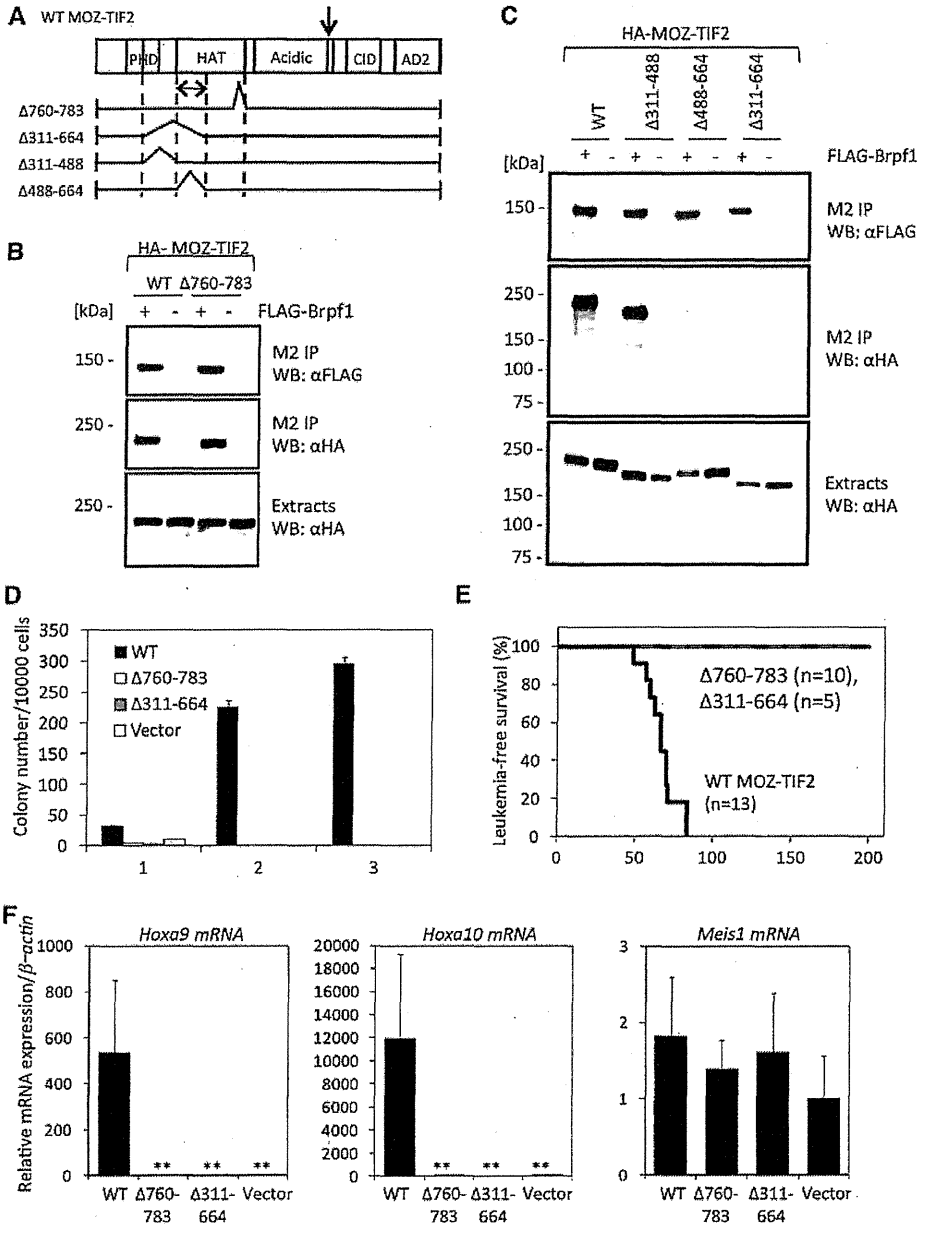

Fig. 2 Interacting domain of MOZ–TIF2 with Brpf1. **a** Structure of MOZ–TIF2 and its deletion mutants. **b** HA-tagged WT or Δ760–783 MOZ–TIF2 was cotransfected into 293FT cells together with FLAG-tagged Brpf1. Immunoprecipitates with anti-FLAG antibody (M2 IP) or cell lysates (Extracts) were subjected to immunoblotting with anti-HA or anti-FLAG antibodies. Both WT and Δ760–783 MOZ–TIF2 interacted with Brpf1. **c** HA-tagged WT or deletion mutants of MOZ–TIF2 were cotransfected into 293FT cells together with FLAG-tagged Brpf1. Immunoprecipitates with anti-FLAG antibody (M2 IP) or cell lysates (Extracts) were subjected to immunoblotting with anti-HA or anti-FLAG antibodies. MOZ–TIF2 containing N-terminal region of MOZ HAT domain (N488–664) interacted with Brpf1. **d** Number of colonies formed by cells transduced with WT, Δ760–783, Δ311–664 MOZ–TIF2 or empty vector. Both of the deletion mutants lost colony formation activity after 2nd round of replating. Data are mean ± SD ($n = 3$). **e** Kaplan–Meier survival curve analysis of mice transplanted with WT, Δ760–783 or Δ311–664 MOZ–TIF2. All of the mice transplanted with WT MOZ–TIF2 developed AML, while all the mice transplanted with deletion mutants of MOZ–TIF2 survived without development of leukemia. **f** First round colonies of cells transduced with WT, Δ760–783, Δ311–664 MOZ–TIF2 or empty vector were collected and analyzed for expression levels of *Hoxa9*, *Hoxa10* and *Meis1* by qRT-PCR analysis. Increased expression levels of *Hoxa9* and *Hoxa10* were only observed in cells transduced with WT MOZ–TIF2. Data are mean ± SD ($n = 3$). $^{**}P < .01$

immunoblotting to determine the knockdown level of *Brpf1* or chromatin immunoprecipitation (ChIP) assay.

Quantitative real-time PCR (qRT-PCR) analysis

Total RNA was extracted using the RNeasy Mini Kit (Qiagen). The cDNA was reverse-transcribed using Superscript® VILO™ (Invitrogen). Expression levels of genes were detected using the ABI 7500 Fast Real-Time PCR System with TaqMan® Gene Expression Assay Mixes (Applied Biosystems). β-actin was used as an internal control.

Immunoprecipitation and western blotting

For immunoprecipitation experiments, certain plasmids were co-transfected into 293FT cells by $CaPO_4$ co-precipitation. Cells were lysed in a lysis buffer [250 mM NaCl, 20 mM sodium phosphate (pH 7.0), 30 mM sodium pyrophosphate, 10 mM NaF, 0.1 % NP-40, 5 mM DTT, 1 mM PMSF, and protease inhibitor cocktail (Roche)], and cell lysates were incubated with anti-FLAG antibody-conjugated agarose beads (Sigma). After rotation at 4 °C overnight, and washing with lysis buffer, precipitated proteins were eluted by FLAG peptide and dissolved with SDS sample buffer. The blots were probed with anti-FLAG (M2) (Sigma), anti-HA (3F10) (Roche), anti-MOZ [ ], anti-Brpf1 (Sigma-Aldrich), or anti-β actin (clone AC-15) (Sigma) as primary antibodies, and horseradish peroxidase-conjugated secondary antibodies (SouthernBiotech). The bands were detected by chemiluminescence using ECL plus Detection Reagents (Amersham Biosciences).

Histone acetylation assay

Immunoprecipitates with anti-FLAG antibody obtained from 293FT cells transfected with FLAG-tagged WT or mutant MOZ were mixed with 50 mM Tris–HCl (pH 8.0), 10 % glycerol, 1 mM dithiothreitol, 0.5 μl of [^{14}C] acetyl-CoA (50 μCi/ml, Amersham), and 1 μg of histone H2A, H2B, H3 and H4, respectively, and incubated at 30 °C for 1 h. After incubation, the samples were subjected to 15 % sodium dodecyl sulfate-PAGE, and the gels were analyzed for the levels of histone acetylation by BAS-2500 (FUJIFILM).

ChIP assay

Cells were fixed with 1 % formaldehyde for 10 min at room temperature and further incubated with 0.125 M glycine for 5 min to stop cross-linking reaction. Cells were then washed with ice-cold PBS containing protease inhibitor cocktail, centrifuged, and the pellets were lysed in lysis buffer (50 mM HEPES pH 7.5, 150 mM NaCl, 1 mM EDTA, 1 % Triton X-100, 0.1 % sodium deoxycholate, 0.1 % sodium dodecyl sulfate, and protease inhibitor cocktail). The lysates were sonicated until the average DNA fragment length was 200–500 bp, using Branson Sonicator, diluted in 10× dilution buffer (1 % Triton X-100, 2 mM EDTA, 20 mM Tris–HCl pH 8.0, 150 mM NaCl and protease inhibitor cocktail), and incubated with antibodies at 4 °C overnight. On the following day, Dynabeads Protein G (Invitrogen) was added and incubated for another 6 h at 4 °C. The immunoprecipitates were washed twice with low salt buffer (0.1 % SDS, 1 % Triton X-100, 2 mM EDTA, 20 mM Tris–HCl pH 8.0 and 150 mM NaCl), once with high salt buffer (0.1 % SDS, 1 % Triton X-100, 2 mM EDTA, 20 mM Tris–HCl pH 8.0 and 500 mM NaCl) and finally twice with PBS containing 0.1 % Triton X-100. Bound chromatin was eluted in elution buffer (1 % SDS and 0.1 M $NaHCO_3$), and together with input DNA, crosslinking was reversed by overnight incubation at 65 °C with addition of 200 mM NaCl to the elution buffer. The eluted samples were then treated with 10 mM EDTA, 40 mM Tris–HCl (pH 6.5), and proteinase K (Roche) at 45 °C for 2 h. Finally, the immunoprecipitated and input DNA were extracted with phenol/chloroform extraction and ethanol precipitation, and analyzed by qRT-PCR using FastStart Universal SYBR Green Master (Roche) and 7500 Fast Real-Time PCR system.

Primer sequences are as follows.

Hoxa7 promoter:

Forward primer (F)/5′-GAGAGGTGGGCAAAGAGTGG-3′, Reverse primer (R)/5′-CCGACAACCTCATACCTATTCCTG-3′

Hoxa7 coding:

F/5′-CTGGACCTTGATGCTTCTAACT-3′, R/5′-AGCCAGAGAAAGAGGGATTCTA-3′

Hoxa9 promoter:

F/5′-GAGCGGTTCAGGTTTAATGC-3′, R/5′-TGCCTGCTGCAGTGTATCAT-3′

Hoxa9 coding:

F/5′-GGTCCCGTGTGAGGTACATGT-3′, R/5′-CAAAACACCAGACGCTGGAA-3′

Hoxa10 promoter:

F/5′-CGGCCTTTGAGCCATAGGT-3′, R/5′-GCCCGCGATTGATATAAATATGT-3′

Hoxa10 coding:

F/5′-TTCGGGCATCCCACTAAATG-3′, R/5′-GGCCACTCGGGCTGTATG-3′

Hoxa13 promoter:

F/5′-TCCTTGGATGAGCGTTCTCT-3′, R/5′-TGCATGTTAAGTGCCTGCTC-3′

β-actin promoter:

F/5′-GCAGGCCTAGTAACCGAGACA-3′, R/5′-AGTTTTGGCGATGGGTGCT-3′

Myf5 promoter:

F/5′-GGAGATCCGTGCGTTAAGAATCC-3′, R/5′-CGGTAGCAAGACATTAAAGTTCCGTA-3′

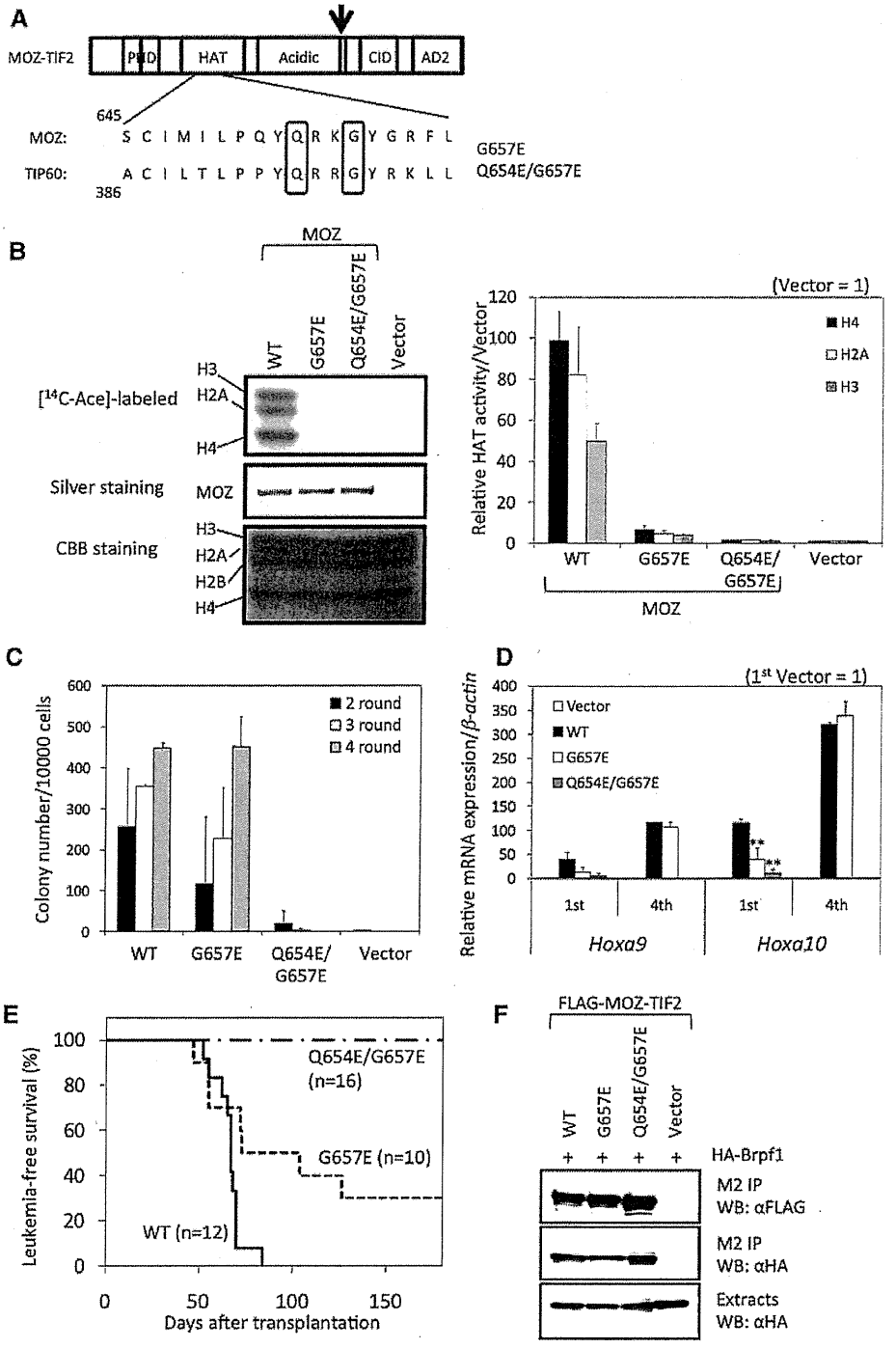

The antibodies used in these experiments are the same as written above for MOZ and Brpf1, and anti-acetyl-Histone H3 (Upstate), and anti-Histone H3 (abcam).

Statistical analysis

Statistical significance was determined by two-tailed Student *t* test.

Results

Brpf1 is required for immortalization of MOZ–TIF2 leukemic cells

Previous studies have suggested that BRPF1 forms complex with MOZ, and interacts directly to MOZ at N-terminal

◀ **Fig. 3** HAT activity of MOZ is required for transformation activity by MOZ–TIF2. **a** Structure of MOZ–TIF2 and its point mutants, Q654E/G657E and G654E. **b** HAT activity of WT and point mutants of MOZ. WT, G654E, Q654E/G657E MOZ or empty vector were cotransfected into 293FT cells. Immunoprecipitates were collected and cultured with histone H2A/B, H3, H4 and C^{14} labeled-acetyl-coenzyme A. C^{14} labeled acetylated histone was detected by BAS. Although HAT activity was reduced in both point mutants of MOZ compared to WT MOZ, G657E MOZ retained subtle HAT activity. Data are mean ± SD ($n = 3$). **c** Colony numbers of cells transduced with WT, G654E, Q654E/G657E MOZ–TIF2 or empty vector. WT and G657E MOZ–TIF2 showed transformation activity, which was not observed in cells transduced with Q654E/G657E MOZ–TIF2 or empty vector. **d** First round and 4th round colonies of cells transduced with WT, G654E, Q654E/G657E MOZ–TIF2 or empty vector were collected and analyzed for expression levels of *Hoxa9, Hoxa10* by qRT-PCR analysis. Expression level of *Hoxa10* was significantly lower in colony cells transduced with both mutants compared to WT MOZ–TIF2 at 1st round, but reached to the similar levels at 4th round in cells with Q654E/G657E MOZ–TIF2. Data are mean ± SD ($n = 3$). $^{**}P < .01$. **e** Kaplan–Meier survival curve analysis of mice transplanted with WT, G657E or Q654E/G657E MOZ–TIF2. All of the mice transplanted with WT MOZ–TIF2 and 7 out of 10 mice transplanted with G657E MOZ–TIF2 developed AML, while none of the mice transplanted with Q654E/G657E MOZ–TIF2 developed leukemia. **f** FLAG-tagged WT, G654E, Q654E/G657E MOZ–TIF2 or empty vector were cotransfected into 293FT cells together with HA-tagged Brpf1. Immunoprecipitates with anti-FLAG antibody (M2 IP) or cell lysates (Extracts) were subjected to immunoblotting with anti-HA or anti-FLAG antibodies. WT and both point mutants of MOZ–TIF2 were able to interact with Brpf1

domain [18]. Thus, we firstly constructed deletion mutant of BRPF1 (Δ1–222) which lacks interacting domain with MOZ, and performed immunoprecipitation assay. This mutant BRPF1 consistently lacked potential to form complex with MOZ (Fig. 1a). Using wild-type (WT) and deletion mutant of BRPF1, we next examined the effect of *Brpf1* knockdown in MOZ–TIF2 leukemic cells. MOZ–TIF2-tranduced mouse BM cells were subsequently transduced with Brpf1 shRNA by lentivirus system. Knockdown efficiencies were confirmed by qRT-PCR and western blotting (Fig. 1b, c). *Brpf1* knockdown resulted in marked decrease of colony numbers, which was rescued by WT human BRPF1 but not by mutant human BRPF1 (Fig. 1d). We further examined the effect of *Brpf1* knockdown on transcriptional activation induced by MOZ–TIF2. As expected, *Brpf1* knockdown led to decrease of *Hoxa9*, *Hoxa10* and *Meis1* expression (Fig. 1E). This decrease was again restored by WT human BRPF1 but not by mutant human BRPF1. These data suggest that Brpf1 contributes to *Hoxa9, Hoxa10* and *Meis1* transcription, which are overexpressed in AML patients with MOZ fusions [15].

Interacting domain of MOZ with Brpf1 is essential for initiation of MOZ–TIF2 leukemia

To investigate the importance of MOZ interaction with Brpf1, we firstly constructed several MOZ–TIF2 mutants as shown in Fig. 2a, and performed immunoprecipitation assay. The 760–783 region of MOZ was previously reported to be the interacting domain with BRPF1 [18]. However, deletion of the region 760–783 did not affect interaction of MOZ–TIF2 with BRPF1 in our condition (Fig. 2b). We previously found that the 760–783 region is required for histone acetyltransferase (HAT) activity [1]. Deletion analysis showed that there is another interacting domain that localized at HAT domain (N488–664) (Fig. 2c). For the following assay, we selected two deletion mutants of MOZ–TIF2, previously reported mutant Δ760–783, and Δ311–664 which lacks the novel interacting domain. We transduced these two deletion mutants, WT MOZ–TIF2 or empty vector to BM progenitors and performed colony formation assay. While WT MOZ–TIF2 cells were capable of forming colonies for several times of replating, others including two deletion mutants of MOZ–TIF2 lost their ability to form colonies in the 2nd round (Fig. 2d). 1st round colony cells were collected and analyzed for expression levels of *Hoxa9*, *Hoxa10* and *Meis1* by qRT-PCR. Corresponding to the results of colony formation assay, transcriptional activation of *Hoxa9* and *Hoxa10* induced by WT MOZ–TIF2 was not observed by two deletion mutants (Fig. 2f). Furthermore, none of the mice injected with BM cells transduced with either of the deletion mutants of MOZ–TIF2 developed AML (Fig. 2e).

HAT activity of MOZ contributes to leukemic transformation induced by MOZ–TIF2

The 760–783 and 488–664 regions were localized in MOZ HAT domain [1]. Although HAT activity is reported to be dispensable for leukemogenesis by MOZ–TIF2 [10], we evaluated the possible association between lack of MOZ HAT activity and loss of leukemogenic potential in Δ311–664 or Δ760–783 mutant MOZ–TIF2. MOZ is the founding member of the MYST family of HATs, which share the conserved MYST domains [5]. To assess the importance of MOZ HAT activity, we constructed previously reported MOZ HAT-deficient G657E mutant as well as Q654E/G657E mutant according to the HAT-deficient mutant of TIP60 (Fig. 3a) [8, 19, 20]. Firstly, we assessed HAT activity of these two HAT-deficient mutants using immunoprecipitates with anti-FLAG antibody, obtained from 293FT cells transfected with FLAG-tagged WT or mutant MOZ (Fig. 3b). WT MOZ showed HAT activity for Histones H2A, H3, H4. Although both HAT-deficient mutants G657E and Q654E/G657E possessed markedly low HAT activity compared to WT MOZ, HAT activity slightly remained in G657E mutant. Next, we examined the colony formation activity of these two HAT-deficient mutants. BM progenitors were transduced with WT, G657E, Q654E/G657E mutant of MOZ–TIF2 or empty vector and subsequently cultured in methylcellulose media. Through 4 rounds of replating, WT and G657E mutant, but not Q654E/G657E mutant, were capable of

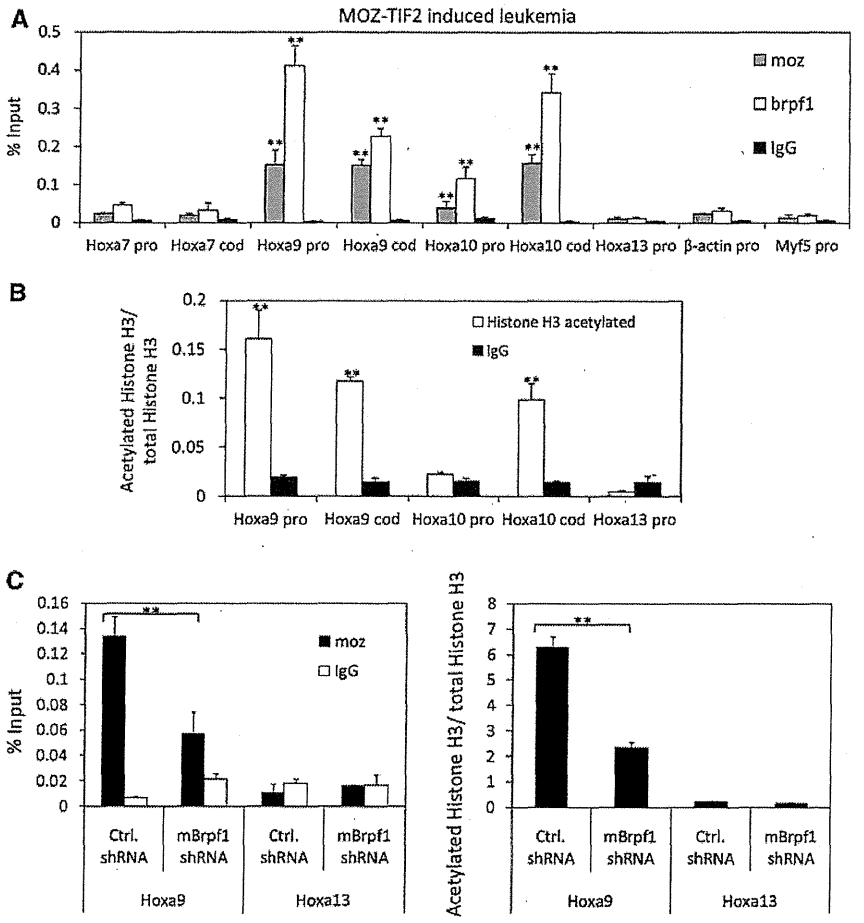

Fig. 4 *Hoxa9* and *Hoxa10* are direct targets of Moz and Brpf1. **a, b** Relative binding of Moz, Brpf1 and acetylated Histone H3 to the promoter and coding region of indicated genes in MOZ–TIF2 leukemic cells. Moz and Brpf1 colocalized at *Hoxa9* and *Hoxa10* genes, in which acetylated Histone H3 levels were higher compared to other tested genes. Data are mean ± SD ($n = 3$). $^{**}P < .01$. **c** Relative binding of Moz and acetylated Histone H3 to the promoter region of *Hoxa9* and *Hoxa13* after *Brpf1* knockdown. Downregulation of Brpf1 reduced the localization of Moz on promoter region of Hoxa9 and also reduced Histone H3 acetylation. Data are mean ± SD ($n = 3$). $^{**}P < .01$

inducing serial replating activity (Fig. 3c). *Hoxa10* expression levels of the 1st round colony cells were decreased by both mutants, but increased to similar level as WT in the 4th round by G657E mutant (Fig. 3d). BM progenitors transduced with WT, G657E or Q654E/G657E mutant of MOZ–TIF2 were also transplanted into sublethally irradiated recipient mice. G657E mutant MOZ–TIF2 led to development of AML in a subset of mice as reported before [8]. However, Q654E/G657E mutant MOZ–TIF2 showed no potential to initiate leukemia (Fig. 3e). These two HAT-deficient mutants were confirmed to be capable of interacting with Brpf1 at similar level as WT MOZ–TIF2 (Fig. 3f). These results indicate that even in a slight level, MOZ HAT activity is required for leukemogenic activity induced by MOZ–TIF2, which was independent of interaction with Brpf1.

Hoxa9 and *Hoxa10* are direct targets of MOZ and BRPF1 complex

To understand the mechanism of leukemic transformation induced by MOZ–TIF2, we performed chromatin immunoprecipitation (ChIP) assay using MOZ–TIF2 colony cells. As shown in Fig. 4a, MOZ and Brpf1 colocalized on chromatin within *Hoxa9* and *Hoxa10* locus, suggesting that these genes are direct targets of MOZ and Brpf1 complex. Indeed, Histone H3 acetylation level was upregulated at target *Hoxa9* and *Hoxa10* genes (Fig. 4b). We also performed ChIP assay using Brpf1 shRNA expressing MOZ–TIF2 colony cells. Depletion of Brpf1 resulted in reduction of MOZ localization on target *Hoxa9* gene, suggesting that Brpf1 enhances the enrichment level of MOZ localization on target genes (Fig. 4c). Together, these data suggest that Brpf1 leads to MOZ localization on the target genes, *Hoxa9* and *Hoxa10*, which enhance histone H3 acetylation and transcriptional activation of these genes, eventually resulting in development of AML.

Hoxa9 overexpression is not substantial for transformation of MOZ–TIF2 in Brpf1 downregulated cells

Previously, HOXA9 alone was reported to be sufficient for leukemic transformation in vitro [11, 13]. Because MOZ–

TIF2 leukemic cells exhibited lower expression level of *Hoxa9*, we assessed the effect of HOXA9 overexpression in MOZ–TIF2 leukemic cells with *Brpf1* knockdown. Unexpectedly, enforced expression of human HOXA9 failed to restore colony formation ability that was impaired by *Brpf1* knockdown (Fig. 5a, b). Downregulation of endogenous *Hoxa9*, *Hoxa10* and *Meis1* by depletion of Brpf1 was not restored by HOXA9 overexpression (Fig. 5c), suggesting again that Brpf1 contributes to transcriptional activation of not only *Hoxa9* but also *Hoxa10* and *Meis1*, both of which do influence the leukemic transformation activity. [12, 14, 21, 22].

Discussion

HOX genes are deregulated in a subset of AML patients, which strongly correlate with poor prognosis [23, 24]. Human AML with MOZ fusions applies to this subset of group, with high levels of *HOXA9* and *HOXA10* [15]. Herein, upregulation of *HOX* genes may contribute to the leukemogenesis in MOZ-related AML. To assess the mechanism and the role of *HOX* genes deregulation in MOZ-related leukemias, we focused on Brpf1. Brpf1, a component of MOZ complex, possesses PHD finger domain, bromodomain and PWWP domain [16, 17, 25]. PWWP domain and bromodomain of Brpf1 directly bind to Histones and are required for chromatin targeting by Brpf1 [16]. Previous study in zebrafish and medaka suggested that Brpf1 is required for the maintenance of *Hox* genes expression through Moz-dependent histone acetylation. [16, 17] Thus, Brpf1 may contribute to upregulation of *HOX* genes in MOZ-related leukemias.

In this study, we have demonstrated that Brpf1 plays an important role in leukemogenesis induced by MOZ–TIF2. Our data indicated that *Hoxa9* and *Hoxa10* were direct

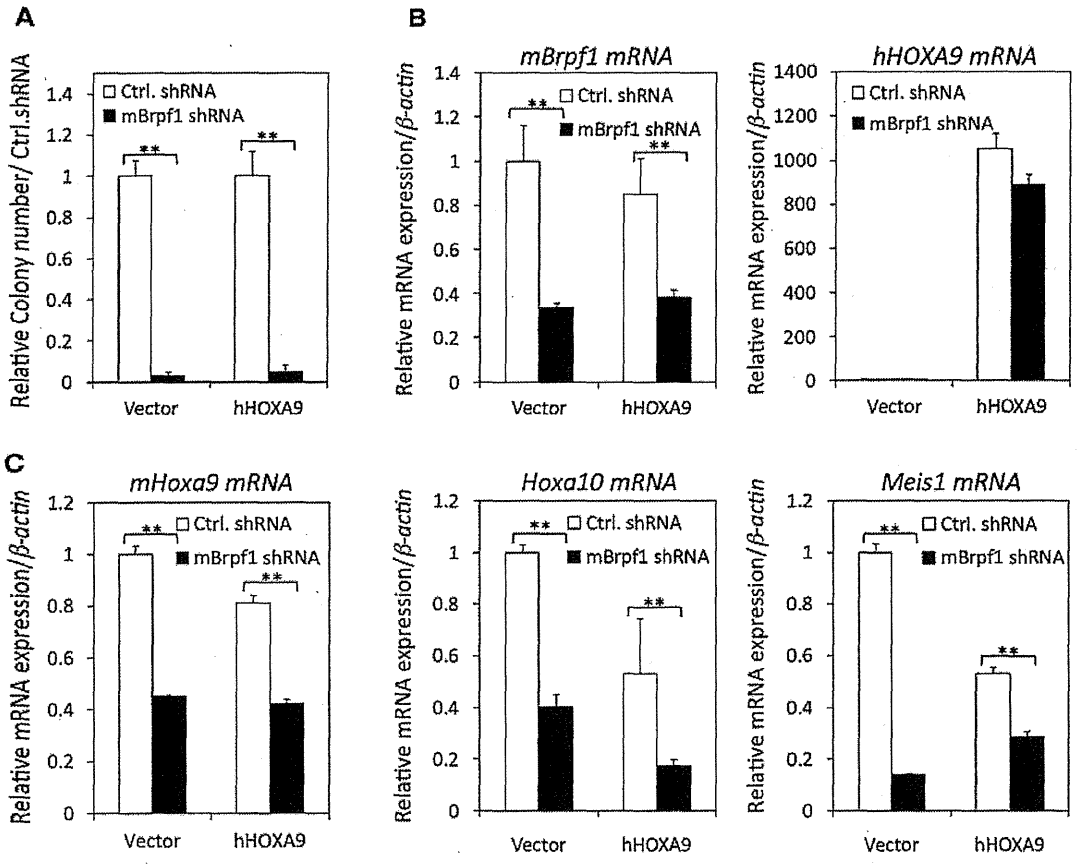

Fig. 5 Effect of HOXA9 overexpression on MOZ–TIF2 leukemic cells with downregulated Brpf1. **a** Relative colony number of MOZ–TIF2 leukemic cells transduced with control shRNA or Brpf1 shRNA. Overexpression of wild-type HOXA9 was not sufficient to restore colony formation activity of MOZ–TIF2 leukemic cells with downregulated Brpf1. Data are mean ± SD ($n = 3$). $^{**}P < .01$. **b** Expression of murine *Brpf1* and human *HOXA9* after Brpf1 shRNA and HOXA9 overexpression. **c** Effects of Brpf1 shRNA and HOXA9 overexpression on expression levels of *Hoxa9*, *Hoxa10* and *Meis1* in Brpf1 downregulated MOZ–TIF2 leukemic cells. Reduced expressions of *Hoxa9*, *Hoxa10* and *Meis1* by *Brpf1* knockdown were sustained in cells with HOXA9 overexpression. Data are mean ± SD ($n = 3$). $^{**}P < .01$

targets of MOZ and BRPF1 in MOZ–TIF2 leukemic cells. Because depletion of Brpf1 exhibited decreased level of MOZ localization on these target genes, resulting in loss of transformation ability induced by MOZ–TIF2, we suggest that Brpf1 promotes MOZ to localize on chromatin of these target genes. Brpf1 recruits MOZ to the target genes and upregulates transcriptional activation through histone H3 acetylation. Since binding of MOZ–TIF2 to the *Meis1* gene locus is weak compared to its binding to *Hoxa9* and *Hoxa10* (data not shown), MOZ–TIF2 is unlikely to regulate the expression of Meis1 directly. Our data also indicate that HAT activity of MOZ is essential for transformation activity induced by MOZ–TIF2. HAT-deficient MOZ–TIF2 was incapable of not only deregulating *Hox* genes, but also initiating leukemia. We suggest that MOZ or MOZ-fusion/BRPF1 complex upregulates *HOX* genes mediated by MOZ-dependent histone acetylation, which finally leads to the development of leukemia.

Although HOXA9 alone possesses transformation activity, enforced expression of human HOXA9 unexpectedly failed to rescue transformation activity abolished by Brpf1 depletion. There are two possible reasons to be considered. Firstly, *Hoxa10* and *Meis1*, both of which were downregulated in Brpf1 depleted cells remained in lower level compared to control cells despite HOXA9 overexpression. This may suggest that downregulation of several *HOX* genes other than *HOXA9* may result in loss of leukemic transformation. Secondly, Brpf1 may be required for HOXA9 function and its downstream pathway. Further study is required to determine the association of Brpf1 and Hoxa9 in the maintenance of transformation activity in AML cells.

Previously, we have shown that upregulation of M-CSFR is critical for the regulation of AML stem cells in MOZ–TIF2 leukemia, and STAT5, which was highly phosphorylated in M-CSFR high cells but not in low cells, may contribute to the clonal expansion and stem cell maintenance [2]. In this study, we demonstrated that deletion mutant of MOZ–TIF2 lacking interacting domain with Brpf1 lost its transformation activity. However, M-CSFR upregulation was maintained in BM cells transduced with this mutant MOZ–TIF2. Furthermore, Hoxa9 expression was upregulated in both M-CSFR-high cells and low cells [2]. Therefore, MOZ/BRPF1/HOX pathway should be considered as independent of PU.1/M-CSFR pathway (Fig. 6). Collectively, our study reveals that MOZ/BRPF1/HOX pathway plays a crucial role in the development of leukemia induced by MOZ–TIF2. For efficient induction of AML, block in the normal hematopoietic differentiation program together with unrestrained growth is required. Several AML-associated chromosomal translocations require additional mutations for the progenitors to gain both of these functions [26, 27]. However, in terms of MOZ–TIF2 leukemia, although increased expression of *HOX* genes may be insufficient to induce AML in a short period, increased phosphorylation of STAT5 mediated by PU.1/M-CSFR pathway would accelerate the development of leukemia. Thus, both MOZ/BRPF1/HOX pathway and PU.1/M-CSFR pathway are essential for the development of MOZ–TIF2 AML.

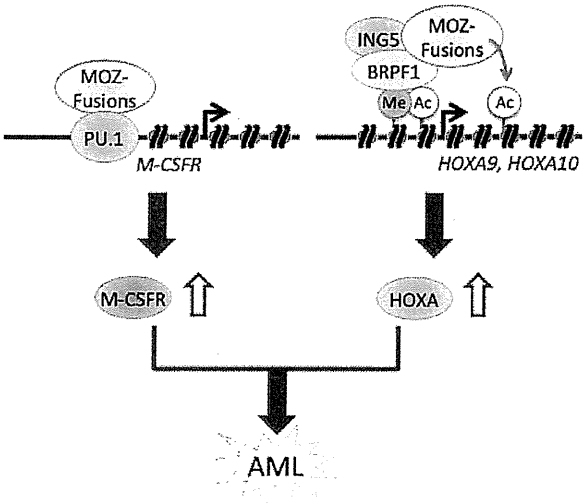

Fig. 6 Model of leukemogenic mechanism induced by MOZ–TIF2. Apart from PU.1/M-CSFR pathway, BRPF1/HOX pathway is essential for leukemogenesis by MOZ–TIF2. BRPF1 enhances the localization of MOZ on target genes such as *HOXA9* or *HOXA10*, and promotes Histone H3 acetylation, which may result in transcriptional upregulation of target genes, finally contributing to the development of leukemia

Acknowledgments This work was supported in part by Grants-in-Aid from the Ministry of Health, Labor, and Welfare; the Ministry of Education, Culture, Sports, Science, and Technology; and National Cancer Center Research and Development Fund.

Conflict of interest The authors declare no competing financial interests.

References

1. Kitabayashi I, Aikawa Y, Nguyen LA, et al. Activation of AML1-mediated transcription by MOZ and inhibition by the MOZ–CBP fusion protein. EMBO J. 2001;20(24):7184–96.
2. Aikawa Y, Katsumoto T, Zhang P, et al. PU.1-mediated upregulation of CSF1R is crucial for leukemia stem cell potential induced by MOZ–TIF2. Nat Med. 2010;16(5):580–5.
3. Rokudai S, Aikawa Y, Tagata Y, et al. Monocytic leukemia zinc finger (MOZ) interacts with p53 to induce p21 expression and cell-cycle arrest. J Biol Chem. 2009;284(1):237–44.
4. Katsumoto T, Aikawa Y, Iwama A, et al. MOZ is essential for maintenance of hematopoietic stem cells. Genes Dev. 2006;20(10):1321–30.
5. Borrow J, Stanton VP Jr, Andresen JM, et al. The translocation t(8;16)(p11;p13) of acute myeloid leukaemia fuses a putative

acetyltransferase to the CREB-binding protein. Nat Genet. 1996;14:33–41.
6. Kitabayashi I, Aikawa Y, Yokoyama A, et al. Fusion of MOZ and p300 histone acetyltransferases in acute monocytic leukemia with a t(8;22)(p11;q13) chromosome translocation. Leukemia. 2001;15:89–94.
7. Chaffanet M, Gressin L, Preudhomme C, et al. MOZ is fused to p300 in an acute monocytic leukemia with t(8;22). Genes Chromosomes Cancer. 2000;28:138–44.
8. Deguchi K, Ayton PM, Carapeti M, et al. MOZ–TIF2-induced acute myeloid leukemia requires the MOZ nucleosome binding motif and TIF2-mediated recruitment of CBP. Cancer Cell. 2003;3:259–71.
9. Yang XJ, Ullah M. MOZ and MORF, two large MYSTic HATs in normal and cancer stem cells. Oncogene. 2007;26:5408–19.
10. Carapeti M, Aguiar RC, Goldman JM, et al. A novel fusion between MOZ and the nuclear receptor coactivator TIF2 in acute myeloid leukemia. Blood. 1998;91:3127–33.
11. Calvo KR, Sykes DB, Pasillas M, Kamps MP. Hoxa9 immortalizes a granulocyte macrophage colony stimulating factor dependent promyelocyte capable of biphenotypic differentiation to neutrophils or macrophages independent of enforced Meis expression. Mol Cell Biol. 2000;20:3274–85.
12. Buske C, Feuring-Buske M, Antonchuk J, et al. Overexpression of HOXA10 perturbs human lymphomyelopoiesis in vitro and in vivo. Blood. 2001;97:2286–92.
13. Thorsteinsdottir U, Mamo A, Kroon E, et al. Overexpression of the myeloid leukemia associated Hoxa9 gene in bone marrow cells induces stem cell expansion. Blood. 2002;99:121–9.
14. Thorsteinsdottir U, Sauvageau G, Hough MR, et al. Overexpression of HOXA10 in murine hematopoietic cells perturbs both myeloid and lymphoid differentiation and leads to acute myeloid leukemia. Mol Cell Biol. 1997;17:495–505.
15. Camós M, Esteve J, Jares P, et al. Gene expression profiling of acute myeloid leukemia with translocation t(8;16)(p11;p13) and MYST3-CREBBP rearrangement reveals a distinctive signature with a specific pattern of HOX gene expression. Cancer Res. 2006;66(14):6947–54.
16. Hibiya K, Katsumoto T, Kondo T, et al. Brpf1, a subunit of the MOZ histone acetyl transferase complex, maintains expression of anterior and posterior Hox genes for proper patterning of craniofacial and caudal skeletons. Dev Biol. 2009;329(2):176–90.
17. Laue K, Daujat S, Crump JG, et al. The multidomain protein Brpf1 binds histones and is required for Hox gene expression and segmental identity. Development. 2008;135:1935–46.
18. Ullah M, Pelletier N, Xiao L, et al. Molecular architecture of quartet MOZ/MORF histone acetyltransferase complexes. Mol Cell Biol. 2008;28(22):6828–43.
19. Ikura T, Ogryzko VV, Grigoriev M, et al. Involvement of the TIP60 histone acetylase complex in DNA repair and apoptosis. Cell. 2000;102(4):463–73.
20. Perez-Campo FM, Borrow J, Kouskoff V, Lacaud G. The histone acetyl transferase activity of monocytic leukemia zinc finger is critical for the proliferation of hematopoietic precursors. Blood. 2009;113(20):4866–74.
21. Thorsteinsdottir U, Kroon E, Jerome L, et al. Defining roles of Hox and MEIS1 genes in induction of acute myeloid leukemia. Mol Cell Biol. 2001;21(1):224–34.
22. Kroon E, Krosl J, Thorsteinsdottir U, et al. Hoxa9 transforms primary bone marrow cells through specific collaboration with Meis1a but not Pbx1b. EMBO J. 1998;17(13):3714–25.
23. Golub TR, Slonim DK, Tamayo P, et al. Molecular classification of cancer: class discovery and class prediction by gene expression monitoring. Science. 1999;286:531–7.
24. Andreeff M, Ruvolo V, Gadgil S, et al. HOX expression patterns identify a common signature for favorable AML. Leukemia. 2008;22(11):2041–7.
25. Vezzoli A, Bonadies N, Allen MD, et al. Molecular basis of histone H3K36me3 recognition by the PWWP domain of Brpf1. Nat Struct Mol Biol. 2010;17(5):617–9.
26. Naoe T, Kiyoi H. Gene mutations of acute myeloid leukemia in the genome era. Int J Hematol. 2013;97(2):165–74.
27. Shima Y, Kitabayashi I. Deregulated transcription factors in leukemia. Int J Hematol. 2011;94(2):134–41.

Cancer Science
Japanese Cancer Association JCA
Open Access

Nuclear export signal within CALM is necessary for CALM-AF10-induced leukemia

Mai Suzuki,[1] Kazutsune Yamagata,[1] Mika Shino,[1] Yukiko Aikawa,[1] Koichi Akashi,[2] Toshio Watanabe[3] and Issay Kitabayashi[1]

[1]Division of Hematological Malignancy, National Cancer Center Research Institute, Tokyo; [2]Department of Medicine and Biosystemic Science, Kyushu University Graduate School of Medical Science, Fukuoka; [3]Department of Biological Science, Graduate School of Humanities and Sciences, Nara Women's University, Nara, Japan

Key words
AF10, chromosome translocation, histone modification, leukemia, nuclear export signal

Correspondence
Issay Kitabayashi, Division of Hematological Malignancy, National Cancer Center Research Institute, Tsukiji 5-1-1, Chuo-ku, Tokyo 104-0045, Japan.
Tel: +81-3-3542-2511; Fax: +81-3-3542-0688;
E-mail: ikitabay@ncc.go.jp

Funding Information
Ministry of Health, Labor, and Welfare. Ministry of Education, Culture, Sports, Science, and Technology. National Cancer Center Research and Development Fund. Naito Foundation. Cosmetology Research Foundation. Nara Women's University Intramural Grant for Project Research.

Received September 16, 2013; Revised December 5, 2013; Accepted December 30, 2013

Cancer Sci **105** (2014) 315–323

doi: 10.1111/cas.12347

The CALM–AF10 fusion gene, which results from a t(10;11) translocation, is found in a variety of hematopoietic malignancies. Certain HOXA cluster genes and MEIS1 genes are upregulated in patients and mouse models that express CALM-AF10. Wild-type clathrin assembly lymphoid myeloid leukemia protein (CALM) primarily localizes in a diffuse pattern within the cytoplasm, whereas AF10 localizes in the nucleus; however, it is not clear where CALM-AF10 acts to induce leukemia. To investigate the influence of localization on leukemogenesis involving CALM-AF10, we determined the nuclear export signal (NES) within CALM that is necessary and sufficient for cytoplasmic localization of CALM-AF10. Mutations in the NES eliminated the capacity of CALM-AF10 to immortalize murine bone-marrow cells in vitro and to promote development of acute myeloid leukemia in mouse models. Furthermore, a fusion of AF10 with the minimal NES can immortalize bone-marrow cells and induce leukemia in mice. These results suggest that during leukemogenesis, CALM-AF10 plays its critical roles in the cytoplasm.

The chromosome translocation t(10;11)(p13;q14), found in T-cell acute lymphoblastic leukemia (T-ALL), acute myeloid leukemia (AML) and malignant lymphomas, results in the fusion of the clathrin assembly lymphoid myeloid leukemia protein (*CALM*) and *AF10* [1,2]. The CALM–AF10 fusion protein consists of almost all CALM and AF10 proteins, with the exception of one or two plant homeodomain (PHD).[1,3] AF10, also known as MLLT10, interacts with the transcription factor Ikaros and H3K4me3 through its octapeptide motif–leucine zipper (OM-LZ) region and PHD domains, respectively.[4–6] In both mice and humans, CALM-AF10 upregulates certain *HOXA* cluster genes (*HOXA5*, *HOXA7*, *HOXA9* and *HOXA10*) and *MEIS1*.[7,8] *Hoxa5* upregulation, which is critical for CALM-AF10-induced leukemogenesis,[9,10] is mediated by an interaction between the AF10 OM-LZ region and the histone methyltransferase DOT1L, resulting in H3K79 hypermethylation at the *Hoxa5* locus.[9] These findings suggest that CALM-AF10 might function in the nucleus.

The CALM protein shuttles between the cytoplasm and the nucleus under the control of a CRM1-dependent nuclear export signal (NES).[11] In contrast to AF10, which localizes in the nucleus,[4] CALM-AF10 primarily localizes in the cytoplasm.[6,9] Other fusion partners of AF10 in acute myeloid and lymphoid leukemias include MLL, DDX3 and HNRNPH1.[12,13] MLL and hnRNPH1 primarily localize in the nucleus,[14,15] whereas DDX3, like CALM, is mostly distributed throughout the cytoplasm.[16,17] These observations prompted us to investigate whether CALM-AF10 exerts its function in the nucleus or the cytoplasm. We found that mutant CALM-AF10 lacking the NES localized in the nucleus and lost its ability to induce leukemia in mice. Conversely, a fusion consisting of the minimal NES and AF10 localized in the cytoplasm and induced leukemia. These results indicate that the cytoplasmic location of CALM-AF10 is critical for its role in leukemogenesis.

Materials and Methods

Generation of *CALM-AF10* mutant constructs. Plasmid encoding pcDNA3β-FLAG-CALM-AF10 was a gift from Y. Zhang (Department of Biochemistry and Biophysics, University of North Carolina).[9] Plasmid encoding the NES-deficient mutant FLAG-CALM^{NES4A}-AF10 and FLAG-CALM^{NES4A} were generated by introducing four point mutations into the CALM NES sequence by inverse PCR using a site-specific mutagenesis kit (Toyobo, Osaka, Japan).[18] Specifically, leucine (L)-544, L-547, L-551 and isoleucine (I)-553 in the putative NES sequence within CALM-AF10 were replaced by alanine (A), using the following primers: L544A, 5′-GCAGCCAACCTTGTGG

GCAATCTTGGC-3′, and 5′-AGATGAATCCAAGTCATCAGA TACT-3′; L547A, 5′-GCTGTGGGCAATCTTGGCATCGGAA AT-3′, and 5-′GTTGGCTGCAGATGAATCCAAGTCA-3′; L551A, 5′-GCTGGCATCGGAAATGGAACCACTAAG-3′, and 5′-ATT GCCCACAGCGTTGGCTGCAGAT-3′; I553A, 5′-GCCGGAAA TGGAACCACTAAGAATGAT-3′, and 5′-GCCAGCATTGCCC ACAGCGTTGGCT-3′. All mutations were confirmed by DNA sequencing. The AF10 sequence encoding amino acids 81–1027 (mAF10) was amplified by PCR and cloned into pcDNA3β-FLAG. To generate the fusion of the minimal NES with AF10, NES1 (amino acids 543–554) or NES2 (amino acids 539–558) within CALM was generated by PCR amplification using FLAG-CALM-AF10 as a template, and then cloned into pcDNA3β-FLAG-mAF10. The pMY-IG-FLAG-CALM-AF10-IRES-GFP, pMY-IG-FLAG-CALM^{NES4A}-AF10-IRES-GFP, pMY-IG-FLAG-mAF10-IRES-GFP and pMY-IG-FLAG-NES2-AF10-IRES-GFP constructs were generated by inserting the corresponding cDNA into the pMY-IG/IRES-GFP vector.

Cell culture and transfection. COS-7 cells were maintained in DMEM supplemented with 10% FBS, 100 U/mL penicillin, 100 μg/mL streptomycin and 2 mM L-glutamine at 37°C in a humidified 5% CO_2 incubator. COS-7 cells were transfected with pcDNA3β-FLAG constructs using the Effectene Transfection Reagent (Qiagen, Hilden, Germany).

Immunofluorescence analysis. Forty-eight hours after transfection, COS-7 cells transfected with pcDNA3β-FLAG constructs were fixed with 3.7% formaldehyde in PBS and examined by immunofluorescence staining with anti-FLAG M2 monoclonal antibody (Sigma-Aldrich, St. Louis, MO, USA), followed by secondary Alexa Fluor 488-conjugated goat anti-mouse IgG (Invitrogen, Carlsbad, CA, USA). Stained cells were mounted in VECTASHIELD mounting medium and observed using a BX50 fluorescence microscope (Olympus, Tokyo, Japan). Cytospins of murine bone-marrow cells transduced with pMY-IG/IRES-GFP viral constructs encoding FLAG-CALM-AF10, FLAG-CALM^{NES4A}-AF10, FLAG-NES2-AF10 or FLAG-mAF10 were fixed with 4% paraformaldehyde and stained with anti-FLAG M2 monoclonal antibody (Sigma-Aldrich) and anti-KMT4/DOT1L polyclonal rabbit antibody (Abcam, Cambridge, MA, USA), followed by secondary Alexa Fluor 568-conjugated goat anti-mouse IgG (Invitrogen) and Alexa Fluor 488-conjugated goat anti-rabbit IgG (Invitrogen), respectively. Stained bone-marrow cells were mounted in VECTASHIELD mounting medium with DAPI (Vector Laboratories, Burlingame, CA, USA) or Prolong Gold (Invitrogen) and observed under a BZ-9000 fluorescence microscope (Keyence Corporation, Osaka, Japan) or a FluoView FV10i confocal laser scanning microscopy (Olympus).

Retroviral infection and bone-marrow transplantation. C57BL/6J mice were purchased from CLEA Japan (Tokyo, Japan). All mouse experiments were approved by the National Cancer Center Animal Ethics Committee and performed in accordance with the institutional guidelines. The pMY-IG/IRES-GFP constructs encoding FLAG-CALM-AF10, FLAG-CALM^{NES4A}-AF10, FLAG-NES2-AF10 or FLAG-mAF10 were transfected into PLAT-E cells using the GeneJuice transfection reagent (Novagen, Nottingham, UK), and retrovirus supernatants were collected 48 h after transfection. c-kit$^+$ cells (1×10^5 cells), selected from murine total bone-marrow cells using CD117 MicroBeads (Miltenyi Biotec, Bergisch Gladbach, Germany), were incubated with the retrovirus and RetroNectin (Takara Bio, Madison, WI, USA) for 24 h in StemPro-34 SFM medium (Invitrogen) containing cytokines (20 ng/mL SCF, 10 ng/mL IL-6 and 10 ng/mL IL-3). The transduced donor bone-marrow cells were then transplanted into lethally irradiated (9.5 Gy) 7–8-week-old female C57BL/6J recipient mice by intravenous injection. For secondary transplants, bone-marrow cells from the primary leukemia mice were intravenously injected into sub-lethally irradiated (6 Gy) female C57BL/6J mice.

Serial-replating assay. Bone-marrow cells transduced with pMY-IG/IRES-GFP constructs encoding FLAG-CALM-AF10, FLAG-CALM^{NES4A}-AF10, FLAG-NES2-AF10 or FLAG-mAF10 were cultured for 3 days in methylcellulose medium (MethoCult M3234; StemCell Technologies, Vancouver, Canada) supplemented with murine SCF, IL-3 and GM-CSF. The GFP$^+$ cells in methylcellulose medium were then sorted using a JSAN cell sorter (Bay Bioscience, Kobe, Japan) and replated every 3–4 days in methylcellulose medium; colonies and cells were counted at each passage. Cells from the second-round and fifth-round colonies were harvested and analyzed by real-time PCR (RT-PCR).

Real time-PCR analysis. Total RNA from replating colonies was purified using an RNeasy Mini Kit (Qiagen). Purified RNA were reverse-transcribed into cDNA using the High Capacity cDNA Reverse Transcription Kit (Applied Biosystems, Foster City, CA, USA). Real-time PCR was performed using the 7500 Fast Real-time PCR System (Applied Biosystems) using the FastStart Universal Probe Master with ROX (Roche, Basel, Switzerland) and the following TaqMan probes (Applied Biosystems): *Hoxa5* (Mm04213381_s1), *Hoxa7* (Mm00657963_m1), *Hoxa9* (Mm00439364_m1), *Hoxa10* (Mm00433966_m1) and *Meis1* (Mm00487664_m1). The relative expression levels of these genes were normalized against the level of *Actb* (Mm00607939_s1).

Flow-cytometry analysis. Bone-marrow cells from leukemic mice were pre-incubated with rat IgG (Sigma-Aldrich), and then incubated on ice with the appropriate staining reagents: anti-CD115(CSF1R)-PE (eBioscience, San Diego, CA, USA), anti-Mac-1(M1/70)-PE-Cy7 (eBioscience), anti-Gr-1(RB6-8C5)-APC (BD Pharmingen, San Diego, CA, USA) and anti-c-Kit(2B8)-APC-eF780 (eBioscience). FACS analysis and cell sorting were performed using the JSAN cell sorter and the results were analyzed using the FLOWJO software (Tree Star, Standford, CA, USA).

Results

The nuclear export signal within CALM is required for cytoplasmic localization of CALM-AF10. To investigate the role of subcellular localization of CALM-AF10 in leukemogenesis, we focused on the NES within the CALM portion of the fusion protein (amino acids 543–554 of CALM).[9] We generated NES-deficient mutants CALM^{NES4A}-AF10 and CALM^{NES4A}, in which leucine-544, leucine-547, leucine-551 and isoleucine-553 in the putative NES region within CALM were substituted with alanines (NES4A) (Fig. 1a). Expression vectors for FLAG-tagged CALM-AF10, CALM, CALM^{NES4A}-AF10, CALM^{NES4A} and mAF10 (the AF10 portion of CALM-AF10) were transiently transfected into COS-7 cells. Immunofluorescence analysis revealed that CALM and CALM-AF10 primarily localized in the cytoplasm, whereas mAF10 and the NES mutants CALM^{NES4A}-AF10 and CALM^{NES4A} localized in the nucleus (Fig. 1b,c).

To determine the minimal NES, two sequences, NES1 (aa. 543–554) and NES2 (aa. 539–558), were fused to AF10 (Fig. 1a,b). As with mAF10, NES1-AF10 was in the nucleus; by contrast, NES2-AF10 was in the cytoplasm (Fig. 1d). The same results were obtained when these fusion proteins were transduced into murine hematopoietic progenitor cells by retro-

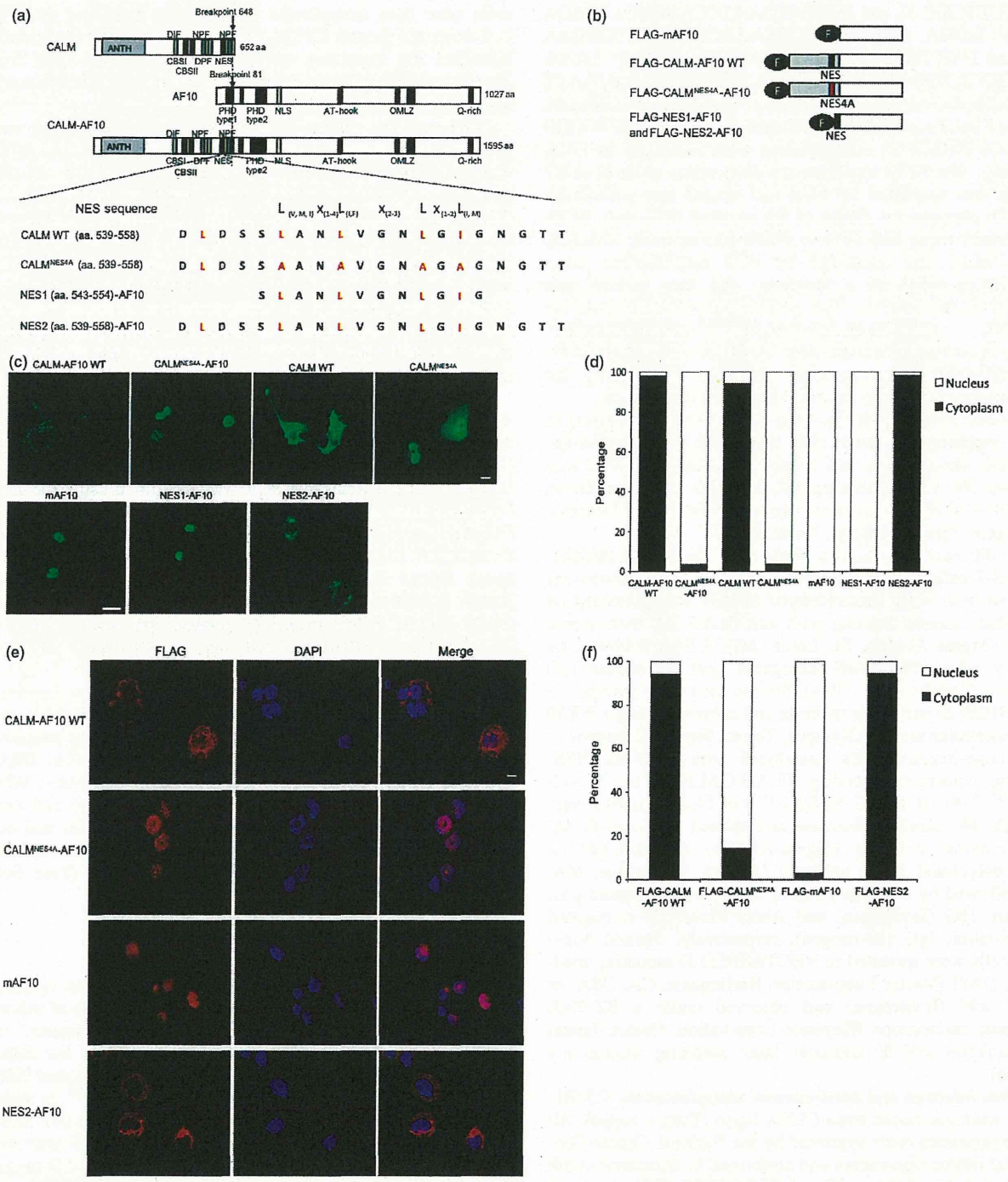

Fig. 1. The NES region within clathrin assembly lymphoid myeloid leukemia protein (CALM) is necessary for cytoplasmic localization. (a) Schematic representations of CALM, AF10, CALM-AF10 and mutant proteins. FLAG-CALM^{NES4A}-AF10 and FLAG-CALM^{NES4A} were generated by alanine substitution of three leucine residues and one isoleucine residue in the putative CALM NES (red). FLAG-NES1-AF10 and FLAG-NES2-AF10 mutants were constructed by fusion of the NES sequences of CALM to the AF10 portion of CALM-AF10. (b) Diagrams of the plasmid constructs used in transfection experiments. (c) Subcellular distribution of CALM-AF10 and the NES point mutations FLAG-CALM-AF10, FLAG-CALM, FLAG-CALM^{NES4A}-AF10, FLAG-CALM^{NES4A}, and FLAG-NES1-AF10, FLAG-NES2-AF10 and FLAG-mAF10 in COS-7 cells. Transfected cells were stained with anti-FLAG antibody (green) and observed by fluorescence microscopy. (d) Population of cells expressing transduced genes in the nucleus and cytoplasm shown in (c). (e) Subcellular distribution of CALM-AF10 and NES mutation proteins in murine bone-marrow cells. Transduced cells were stained with anti-FLAG antibody (red). (f) Population of cells expressing transduced genes in the nucleus and the cytoplasm shown in (e). Nuclei were stained with DAPI (blue) and observed by fluorescence microscopy. The scale bar represents 20 μm in (c) and 10 μm in (e). ANTH, AP180 N-terminal homology domain binding phosphatidylinositol 4,5-bisphosphate (PIP_2); DIF and DPF, motifs interacts with AP-2; NPF, a motif interacts with the EH (Eps15 homology) domain; CBS-I and -II, putative type I and II clathrin-binding sequences; NES, nuclear export signal; PHD Type1 and 2, plant homeodomain zinc finger domains; NLS, nuclear localization signal; AT-hook, DNA-binding protein motif; OMLZ, octapeptide motif-leucine zipper domain; Q-rich, glutamine-rich region.

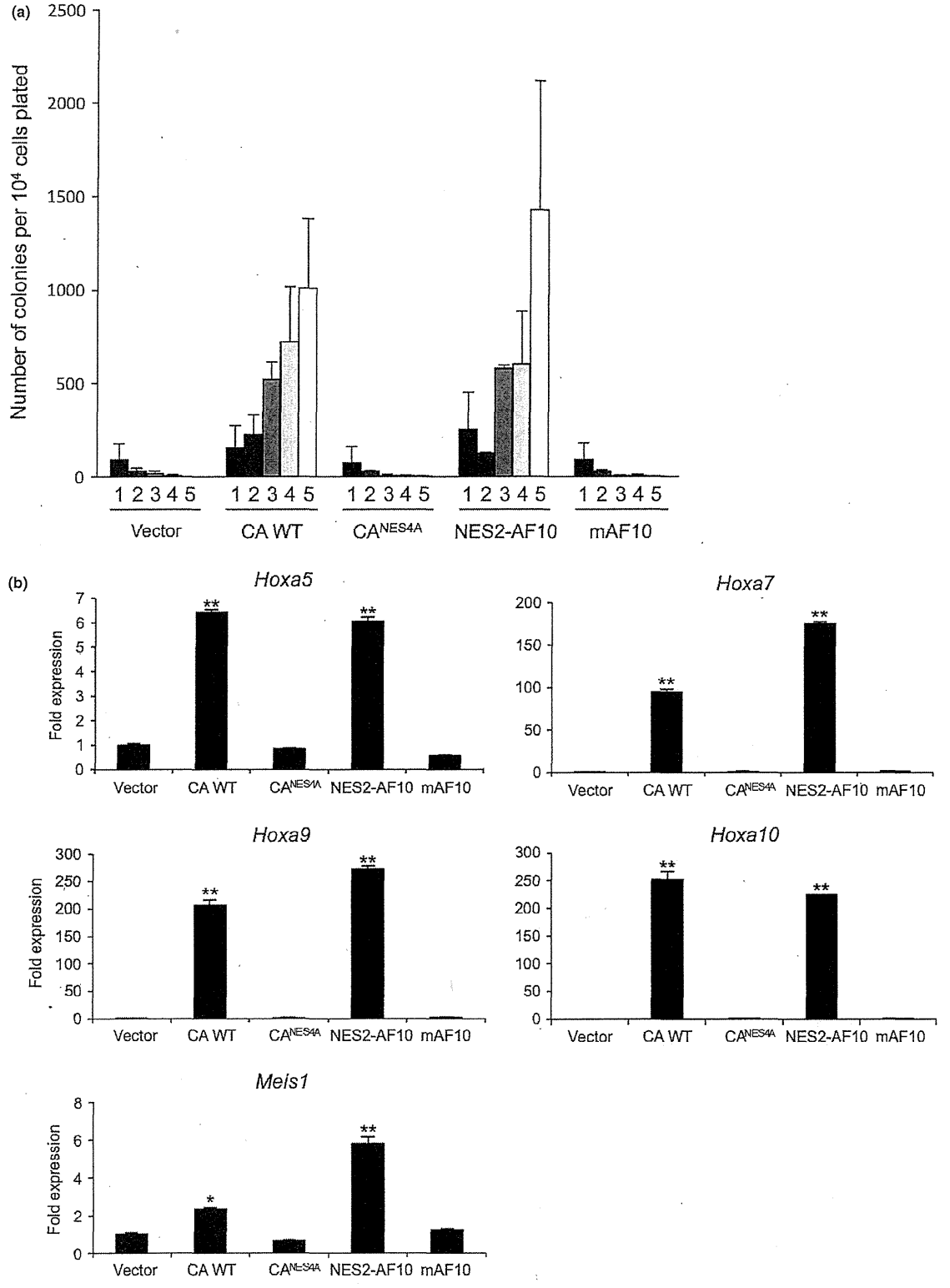

Fig. 2. The nuclear export signal within clathrin assembly lymphoid myeloid leukemia protein (CALM) is critical for *in vitro* immortalization of cells by CALM-AF10. (a) Serial colony-replating assays of murine bone-marrow cells transduced with FLAG-tagged wild-type and mutant CALM-AF10. In each round of replating, 3×10^4 transduced bone-marrow cells were plated. Bars represent the numbers of colonies. (b) *Hoxa* cluster and *Meis1* expression in cells transduced with wild-type or mutant CALM-AF10. RNA transcripts were analyzed by real-time PCR of murine bone-marrow cells transduced with wild-type and mutant CALM-AF10 *in vitro*. Expression levels of *Hoxa5*, *Hoxa7*, *Hoxa9*, *Hoxa10* and *Meis1* were normalized against *Actb* expression and compared with the levels in vector-transfected whole bone-marrow cells. Data are shown as means ± SEM from three independent samples. $^*P < 0.05$; $^{**}P < 0.01$. (*vs* normal bone-marrow cells). CA WT, wild-type CALM-AF10.

viral infection (Fig. 1e). These results indicate that NES1 is not sufficient, but its flanking regions including leucine-540 are necessary for cytoplasmic localization of CALM-AF10. Thus, we concluded that the NES2 region is the minimal NES that mediates cytoplasmic localization of CALM-AF10.

The nuclear export signal within CALM is necessary for CALM-AF10-induced immortalization of cells *in vitro*. We next investigated whether the NES within CALM-AF10 is required for leukemogenesis. To this end, primary murine bone-marrow stem/progenitor cells (HSPC) were infected with retrovirus encoding CALM-AF10, CALM^{NES4A}-AF10, NES2-AF10 and mAF10. Serial-replating assays revealed that both CALM-AF10 and NES2-AF10 immortalized HSPC, and that the cells formed colonies for at least five rounds of replating (Fig. 2a). By contrast, neither mAF10 nor CALM^{NES4A}-AF10, which lacks a functional CALM NES, could immortalize cells. Transduced cells with elevated colony-forming abilities also exhibited upregulation of the *Hoxa* cluster (*Hoxa5*, *Hoxa7*, *Hoxa9* and *Hoxa10*) and *Meis1* genes (Fig. 2b)[7,9]. These results indicated that the CALM NES is necessary for CALM-AF10 to immortalize hematopoietic stem/progenitor cells.

The nuclear export signal within CALM-AF10 is necessary to induce leukemia *in vivo*. To determine whether CALM-AF10 and NES2-AF10 can induce leukemia in mice, we injected bone-marrow progenitor cells transduced with CALM-AF10 and NES2-AF10 into lethally irradiated mice. Seven out of eight mice transplanted with cells expressing CALM-AF10 developed leukemia within 6 months after transplantation (Fig. 3a), and all mice transplanted with cells expressing NES2-AF10 developed leukemia within 3 months after transplantation. When cells prepared from bone marrow of these leukemic mice were transplanted into secondary recipient mice, all recipients promptly developed leukemia (medians: CALM-AF10 donors, 21 days [$n = 4$]; NES2-AF10 donors,

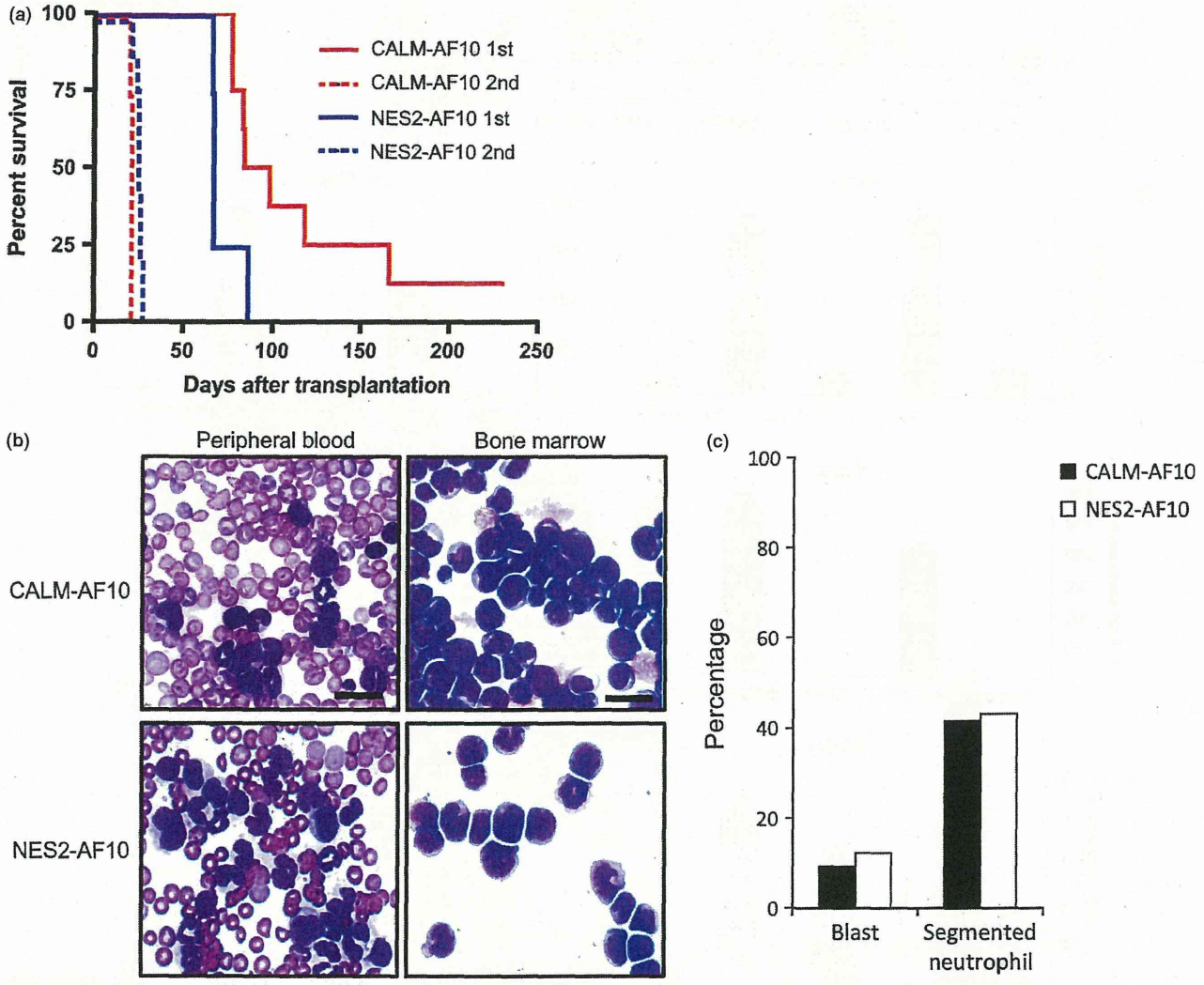

Fig. 3. The nuclear export signal within clathrin assembly lymphoid myeloid leukemia protein (CALM) is sufficient for leukemic transformation by CALM-AF10. (a) Survival of mice injected with murine bone-marrow cells transduced with FLAG-CALM-AF10 or FLAG-NES2-AF10. The leukemia-free survivals of the mice were analyzed. CALM-AF10 primary transplantation, $n = 8$; CALM-AF10 secondary transplantation, $n = 4$; NES2-AF10 primary transplantation, $n = 4$; NES2-AF10 secondary transplantation, $n = 9$. (b) Peripheral blood smears and bone-marrow cytospins were stained with May-Giemsa from CALM-AF10-transduced or NES2-AF10-transduced bone-marrow cells. Original magnification is 400×. (c) Population of blasts and segmented neutrophils in bone-marrow cells shown in (b). The scale bars represent 20 μm.

25 days [$n = 9$]). Morphological analysis revealed large populations of blast cells in leukemic mice receiving cells transduced with either CALM-AF10 or NES2-AF10 (Fig. 3b, c). Flow cytometry analysis showed that cells expressing CALM-AF10 and NES2-AF10 in the bone marrow cells of primary recipient mice were Mac1$^+$, CSF1R$^+$ and c-kit$^+$ (Fig. 4a). Moreover, as shown in Figure 4b, *Hoxa5*, *Hoxa7*, *Hoxa9*, *Hoxa10* and *Meis1* expression levels were upregulated in cells expressing CALM-AF10 and NES2-AF10 compared with normal bone marrow cells, although upregulation of *Hoxa5* and *Meis1* in primary recipient mice harboring NES2-AF10 was not significant ($P = 0.084$ and $P = 0.093$, respectively). These

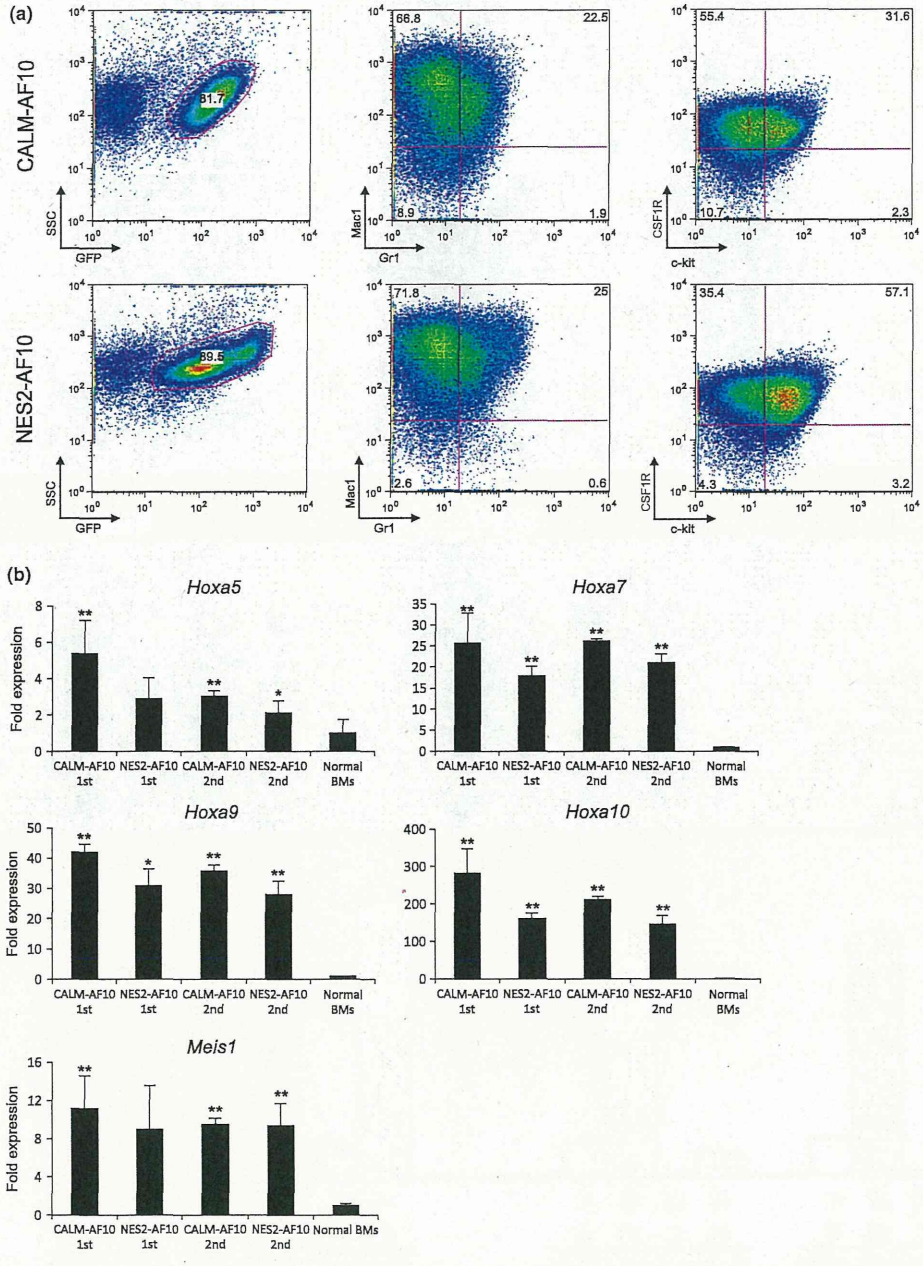

Fig. 4. Characterization of leukemic cells *in vivo*. (a) Flow cytometric analysis of leukemic cells. Murine bone-marrow cells were prepared from mice that developed leukemia after receiving transplantation of tumor cells transduced with CALM-AF10 or NES2-AF10, and were co-stained for Gr-1, Mac-1, colony stimulating factor 1 receptor (CSF1R) and c-kit; data are representative of CALM-AF10 primary transplantation ($n = 3$) and NES2-AF10 primary transplantation ($n = 3$). (b) *Hoxa* cluster and *Meis1* expression in mice receiving cells transduced with wild-type and mutant CALM-AF10. RNA transcripts were analyzed by real-time PCR of bone-marrow cells in mice that developed leukemia after CALM-AF10 and NES2-AF10 bone-marrow transplantation. Expression levels of *Hoxa5*, *Hoxa7*, *Hoxa9*, *Hoxa10* and *Meis1* were normalized against *Actb* and compared with wild-type whole bone marrow. Data are shown as means ± SEM from three independent leukemic mice. $^*P < 0.05$; $^{**}P < 0.01$ (*vs* normal bone-marrow cells).

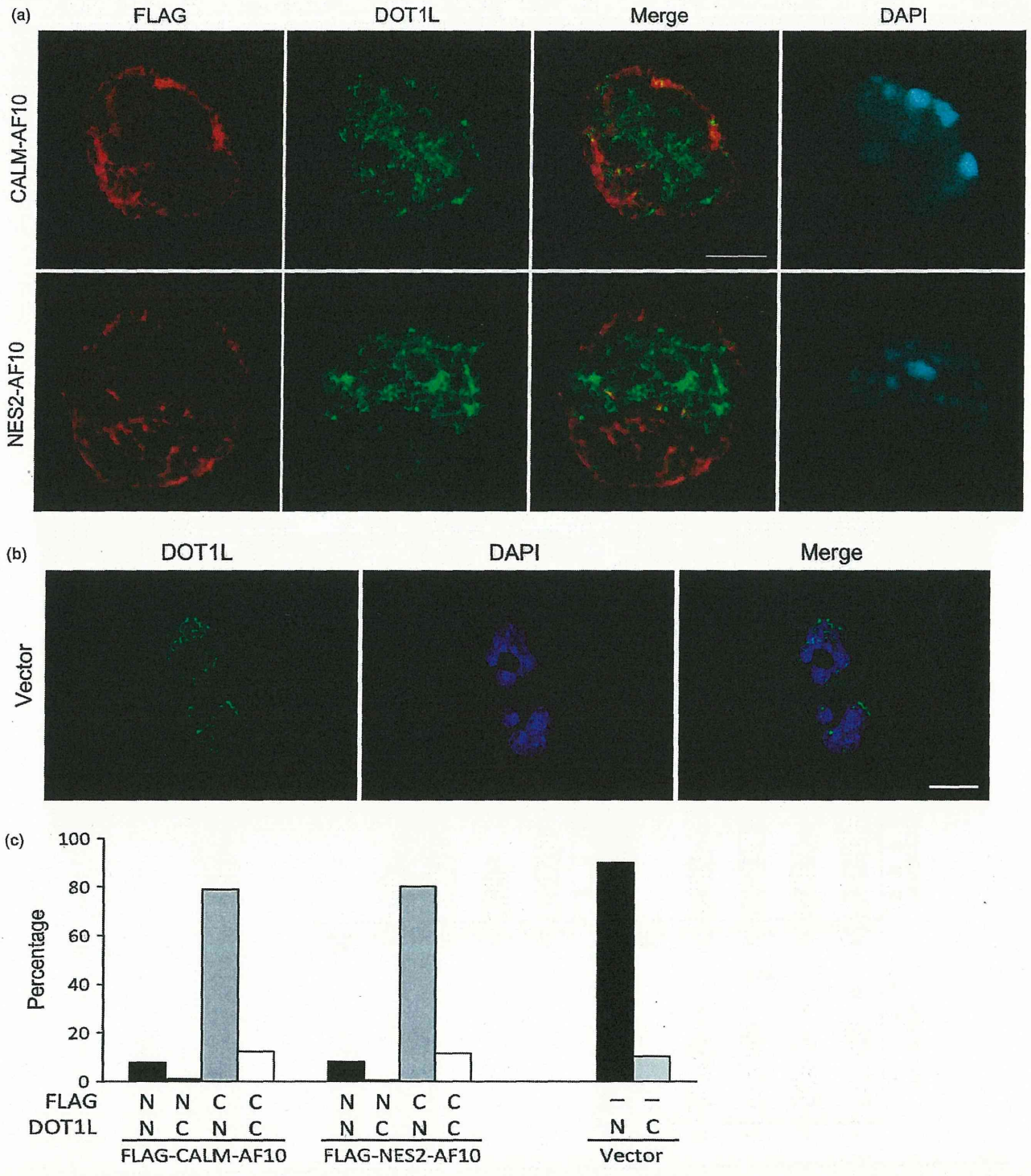

Fig. 5. Dot1L mainly localize in the nucleus in CALM-AF10-induced or NES2-AF10-induced leukemic cells. (a) Subcellular distribution of endogenous Dot1L in CALM-AF10-induced or NES2-AF10-induced leukemic cells. Cytospins of the cells were stained with anti-FLAG antibody (red), anti-DOT1L antibody (green) and DAPI (blue) and observed by confocal laser scanning microscopy. Note that GFP expression was not detected in the condition. (b) Subcellular distribution of endogenous Dot1L in the control vector-infected murine using fluorescence microscopy. (c) Population of leukemia cells expressing DOT1L and CALM-AF10 or FLAG-NES2-AF10 in the nucleus and the cytoplasm shown in (a) and (b). The scale bar represents 5 μm in (a) and 10 μm in (b).

data demonstrate that the NES within CALM-AF10 is a critical element for induction of leukemia.

It has been reported that CALM-AF10 interacts with the histone methyltransferase DOT1L to mediate H3K79 hypermethylation at the *Hoxa5* locus.[9] To determine whether Dot1L colocalizes with CALM-AF10 and NES2-AF10 in the leukemia cells, we performed immunofluorescence analysis. Dot1L mainly localized in the nucleus while CALM-AF10 and NES2-AF10 mainly localized in the cytoplasm (Fig. 5a,b). Dot1L partially colocalized with both CALM-AF10 and NES2-AF10, but neither CALM-AF10 nor NES2-AF10 altered the localization of Dot1L (Fig. 5a).

Discussion

AF10 and CALM localize diffusely in the nucleus and cytoplasm, respectively, whereas CALM-AF10 primarily localizes in cytoplasmic speckle domains (see Fig. 1c,d). The fact that CALM-AF10 regulates histone methylation at the *Hoxa5* locus suggests that CALM-AF10 is likely to function in the nucleus.[9] However, the results described here indicate that the CALM NES is essential for CALM-AF10-induced leukemogenesis, suggesting that cytoplasmic localization (or shuttling between nucleus and cytoplasm) is critical for the function of CALM-AF10. During the preparation of the manuscript, another group reported similar findings,[19] indicating that the results are reproducible and the conclusions can be validated using alternative experimental systems.

The molecular mechanism by which CALM-AF10 exerts its function in the cytoplasm remains unclear, but two possibilities are consistent with the existing data: CALM-AF10 may affect cytoplasmic signaling pathways that regulate expression of its target genes, including *HoxA* cluster genes; alternatively, CALM-AF10 may affect the functions of transcriptional regulators by changing their localization from the nucleus to the cytoplasm. DOT1L, a candidate mediator of CALM-AF10-induced leukemia, interacts with AF10 and induces H3K79 hypermethylation at *Hoxa5*.[9] However, our present data suggest that CALM-AF10 and NES2-AF10 did not affect the localization of Dot1L (see Fig. 5a). It is possible that CALM-AF10 squelches DOT1L inhibitors by exporting them to the cytoplasm.

CALM plays an important role in clathrin-mediated endocytosis.[17,20,21] It and other endocytosis-related genes, such as EPS15, EEN, CLTC and HIP1, are involved in multiple types of leukemia-associated chromosomal translocations (e.g. MLL-CALM, MLL-EPS15, MLL-EEN, CLTC-ALK and HIP1-PDGFBR),[22–26] suggesting that these leukemia-associated fusions might affect endocytosis in a manner that contributes to leukemogenesis. However, recent reports have shown that the clathrin-binding domain of CALM is not essential for CALM-AF10-mediated leukemogenesis.[27,28] Here, we show that nuclear export of CAL-AF10 is critical for the leukemogenesis. Because the endocytosis-related proteins mentioned above are also exported from the nucleus to the cytoplasm, as in the case of CALM,[11,23,29] it is possible that changes in the localization of fusions involving endocytosis-related proteins have some shared consequence that is important for leukemogenesis.

Molecular exchange between the nucleus and cytoplasm takes place through nuclear pore complexes (NPC). Fusion proteins containing NUP98 and NUP214, which are components of the NPC, have been found in AML and T-ALL;[30,31] as in cells expressing CALM-AF10, a set of *Hoxa* and *Meis1* genes are upregulated in leukemia cells expressing these NUP98 fusions and NUP214 fusions.[32,33] In addition, the NPC-component fusions interact with CRM1, the major receptor for the nuclear export of protein.[33,34] These observations suggest that alteration of the localization of certain factors by NUP98 fusions and NUP214 fusions might be important for leukemogenesis, and that a common mechanism may underlie leukemias induced by CALM and NUP fusions.

Acknowledgments

We thank Dr Y. Zhang for pcDNA3β-FLAG-CALM-AF10 plasmid. This work was supported in part by Grants-in-Aid for Scientific Research from the Ministry of Health, Labor, and Welfare and from the Ministry of Education, Culture, Sports, Science, and Technology; the National Cancer Center Research and Development Fund; the Naito Foundation; Cosmetology Research Foundation; and Nara Women's University Intramural Grant for Project Research. MS is a Research Fellow for Yong Scientist of Japan Society for the Promotion of Science.

Disclosure Statement

The authors have no conflict of interest.

References

1 Dreyling MH, MartinezCliment JA, Zheng M, Mao J, Rowley JD, Bohlander SK. The t(10;11)(p13;q14) in the U937 cell line results in the fusion of the AF10 gene and CALM, encoding a new member of the AP-3 clathrin assembly protein family. *Proc Natl Acad Sci USA* 1996; **93**: 4804–9.
2 Bohlander SK, Muschinsky V, Schrader K *et al.* Molecular analysis of the CALM/AF10 fusion: identical rearrangements in acute myeloid leukemia, acute lymphoblastic leukemia and malignant lymphoma patients. *Leukemia* 2000; **14**: 93–9.
3 Narita M, Shimizu K, Hayashi Y *et al.* Consistent detection of CALM-AF10 chimaeric transcripts in haematological malignancies with t(10;11)(p13;q14) and identification of novel transcripts. *Br J Haematol* 1999; **105**: 928–37.
4 Linder B, Newman R, Jones LK *et al.* Biochemical analyses of the AF10 protein: the extended LAP/PHD-finger mediates oligomerisation. *J Mol Biol* 2000; **299**: 369–78.
5 Wysocka J, Swigut T, Xiao H *et al.* A PHD finger of NURF couples histone H3 lysine 4 trimethylation with chromatin remodelling. *Nature* 2006; **442**: 86–90.
6 Greif PA, Tizazu B, Krause A, Kremmer E, Bohlander SK. The leukemogenic CALM/AF10 fusion protein alters the subcellular localization of the lymphoid regulator Ikaros. *Oncogene* 2008; **27**: 2886–96.
7 Caudell D, Zhang Z, Chung YJ, Aplan PD. Expression of a CALM-AF10 fusion gene leads to Hoxa cluster overexpression and acute leukemia in transgenic mice. *Cancer Res* 2007; **67**: 8022–31.
8 Mulaw MA, Krause A, Deshpande AJ *et al.* CALM/AF10-positive leukemias show upregulation of genes involved in chromatin assembly and DNA repair processes and of genes adjacent to the breakpoint at 10p12. *Leukemia* 2012; **26**: 1012–9.
9 Okada Y, Jiang Q, Lemieux M, Jeannotte L, Su L, Zhang Y. Leukaemic transformation by CALM-AF10 involves upregulation of Hoxa5 by hDOT1L. *Nat Cell Biol* 2006; **8**: 1017–24.
10 Chen L, Deshpande AJ, Banka D *et al.* Abrogation of MLL-AF10 and CALM-AF10-mediated transformation through genetic inactivation or pharmacological inhibition of the H3K79 methyltransferase Dot1l. *Leukemia* 2013; **27**: 813–22.
11 Vecchi M, Polo S, Poupon V, van de Loo JW, Benmerah A, Di Fiore PP. Nucleocytoplasmic shuttling of endocytic proteins. *J Cell Biol* 2001; **153**: 1511–7.
12 Borkhardt A, Haas OA, Strobl W *et al.* A novel type of Mll/Af10 fusion transcript in a child with acute megakaryocytic leukemia (Aml-M7). *Leukemia* 1995; **9**: 1796–7.
13 Brandimarte L, Pierini V, Di Giacomo D *et al.* New MLLT10 gene recombinations in pediatric T-acute lymphoblastic leukemia. *Blood* 2013; **121**: 5064–7.

14 Lee JW, Liao PC, Young KC *et al.* Identification of hnRNPH1, NF45, and C14orf166 as novel host interacting partners of the mature hepatitis C virus core protein. *J Proteome Res* 2011; **10**: 4522–34.
15 Ennas MG, Sorio C, Greim R *et al.* The human ALL-1/MLL/HRX antigen is predominantly localized in the nucleus of resting and proliferating peripheral blood mononuclear cells. *Cancer Res* 1997; **57**: 2035–41.
16 Yedavalli VSRK, Neuveut C, Chi YH, Kleiman L, Jeang KT. Requirement of DDX3 DEAD box RNA helicase for HIV-1 Rev-RRE export function. *Cell* 2004; **119**: 381–92.
17 Tebar F, Bohlander SK, Sorkin A. Clathrin assembly lymphoid myeloid leukemia (CALM) protein: localization in endocytic-coated pits, interactions with clathrin, and the impact of overexpression on clathrin-mediated traffic. *Mol Biol Cell* 1999; **10**: 2687–702.
18 Takagi M, Nishioka M, Kakihara H *et al.* Characterization of DNA polymerase from *Pyrococcus* sp. strain KOD1 and its application to PCR. *Appl Environ Microbiol* 1997; **63**: 4504–10.
19 Conway AE, Scotland PB, Lavau CP, Wechsler DS. A CALM-derived nuclear export signal is essential for CALM-AF10-mediated leukemogenesis. *Blood* 2013; **121**: 4758–68.
20 Ford MGJ, Pearse BMF, Higgins MK *et al.* Simultaneous binding of PtdIns (4,5)P-2 and clathrin by AP180 in the nucleation of clathrin lattices on membranes. *Science* 2001; **291**: 1051–5.
21 Meyerholz A, Hinrichsen L, Groos S, Esk PC, Brandes G, Ungewickell EJ. Effect of clathrin assembly lymphoid myeloid leukemia protein depletion on clathrin coat formation. *Traffic* 2005; **6**: 1225–34.
22 Bernard OA, Mauchauffe M, Mecucci C, Vandenberghe H, Berger R. A novel gene, Af-1p, fused to Hrx in T(1,11)(P32, Q23), is not related to Af-4, Af-9 nor Enl. *Oncogene* 1994; **9**: 1039–45.
23 So CW, So CKC, Cheung N, Chew SL, Sham MH, Chan LC. The interaction between EEN and Abi-1, two MLL fusion partners, and synaptojanin and dynamin: implications for leukaemogenesis. *Leukemia* 2000; **14**: 594–601.
24 Bridge JA, Kanamori M, Ma ZG *et al.* Fusion of the ALK gene to the clathrin heavy chain gene, CLTC, in inflammatory myofibroblastic tumor. *Am J Pathol* 2001; **159**: 411–5.
25 Wechsler DS, Engstrom LD, Alexander BM, Motto DG, Roulston D. A novel chromosomal inversion at 11q23 in infant acute myeloid leukemia fuses MLL to CALM, a gene that encodes a clathrin assembly protein. *Genes Chromosom Cancer* 2003; **36**: 26–36.
26 Ross TS, Bernard OA, Berger R, Gilliland DG. Fusion of Huntingtin interacting protein 1 to platelet-derived growth factor beta receptor (PDGF beta R) in chronic myelomonocytic leukemia with t(5;7)(q33;q11.2). *Blood* 1998; **91**: 4419–26.
27 Deshpande AJ, Rouhi A, Lin Y *et al.* The clathrin-binding domain of CALM and the OM-LZ domain of AF10 are sufficient to induce acute myeloid leukemia in mice. *Leukemia* 2011; **25**: 1718–27.
28 Stoddart A, Tennant TR, Fernald AA, Anastasi J, Brodsky FM, Le Beau MM. The clathrin-binding domain of CALM-AF10 alters the phenotype of myeloid neoplasms in mice. *Oncogene* 2012; **31**: 494–506.
29 Engqvist-Goldstein AEY, Kessels MM, Chopra VS, Hayden MR, Drubin DG. An actin-binding protein of the Sla2/Huntingtin interacting protein 1 family is a novel component of clathrin-coated pits and vesicles. *J Cell Biol* 1999; **147**: 1503–18.
30 von Lindern M, Breems D, van Baal S, Adriaansen H, Grosveld G. Characterization of the translocation breakpoint sequences of two DEK-CAN fusion genes present in t(6;9) acute myeloid leukemia and a SET-CAN fusion gene found in a case of acute undifferentiated leukemia. *Genes Chromosom Cancer* 1992; **5**: 227–34.
31 Nakamura T, Largaespada DA, Lee MP *et al.* Fusion of the nucleoporin gene NUP98 to HOXA9 by the chromosome translocation t(7;11)(p15;p15) in human myeloid leukaemia. *Nat Genet* 1996; **12**: 154–8.
32 Nakamura T. NUP98 fusion in human leukemia: dysregulation of the nuclear pore and homeodomain proteins. *Int J Hematol* 2005; **82**: 21–7.
33 Van Vlierberghe P, van Grotel M, Tchinda J *et al.* The recurrent SET-NUP214 fusion as a new HOXA activation mechanism in pediatric T-cell acute lymphoblastic leukemia. *Blood* 2008; **111**: 4668–80.
34 Takeda A, Sarma NJ, Abdul-Nabi AM, Yaseen NR. Inhibition of CRM1-mediated nuclear export of transcription factors by leukemogenic NUP98 fusion proteins. *J Biol Chem* 2010; **285**: 16248–57.